Recent Advancement in Biomedical Application on the Surface of Two-Dimensional Materials: From Biosensing to Tissue Engineering

Emily P. Nguyen[1], Cecilia de Carvalho Castro e Silva[1,2] & Arben Merkoçi[1,3]*

1. Nanobioelectronics &Biosensors Group, Catalan Institute of Nanoscience and Nanotechnology (ICN2), CSIC and BIST, Campus UAB, Bellaterra, 08193, Barcelona, Spain
2. MackGraphe – Graphene and Nanomaterials Research Center, Mackenzie Presbyterian University, 01302-907, São Paulo, Brazil
3. ICREA Institució Catalana de Recerca i Estudis Avançats, Barcelona 08010, Spain
*Email: arben.merkoçi@icn2.cat

Abstract:

As biosensors and biomedical devices become increasingly important to everyday diagnostics and monitoring, there are tremendous, and constant, efforts towards developing and improving the reliability and versatility of such technology. Offering high surface area-to-volume ratios and a diverse range of properties, from electronic to optical, two dimensional (2D) materials have proven to be very promising candidates for biological applications and technologies. Due to the dimensionality, 2D materials facilitates many interfacial phenomena that has shown to significantly improve the performance of biosensors, while recent advances in synthesis techniques and surface engineering methods also enables the realization of future biomedical devices. This short review aims to highlight the influence of 2D material surfaces and the properties that arise due to its 2D structure. Using recent (within the last few years) examples of biosensors and biomedical applications, we emphasize the important role of 2D materials in advancing developments and research for biosensing and healthcare.

1. Introduction

Since the isolation of graphene in 2004[1], 2D materials has revolutionized many aspects of scientific and technological research. In that time, the family of 2D materials has immensely grown to include all different types of lattice configurations (from honeycomb to octahedral) with different atomic compositions and ratios, and exhibit different types of electronic structures (conducting to insulating)[2,3] The advantages of using 2D materials lie predominantly in their 2D structure that, in comparison to their bulk counterparts, exhibits many fascinating and unique properties.[4–6]

One area of research that has benefited greatly from 2D materials is the field of bio-applications. In particular, for biosensing and biomedical devices, tremendous progress and technological advancements have been achieved.[7–9] In the biomedical applications of the 2D materials, the biological species, such as: biomolecules, bioreceptors, cells, tissues and pathogens etc., will be in direct contact with the surface of

these materials. In this way, the successful development of biomedical devices based on 2D materials, lies in understanding the surface properties of these materials and how to harness these properties for many different applications, such as in biosensors, implants, tissue engineering, antimicrobial and antifouling, among others. An example of that, is the integration of 2D materials in biosensors. As most of the atoms for the 2D materials are on the surface, their physical and electronic properties can be more effectively modified with the interaction of bioreceptors and/or biomolecules, making these materials excellent platforms for the development of highly sensitive biosensors.[10–12]

Based on that, in this short review, we aim to explore the surface effects in the current and a few emerging 2D materials and how the surface properties of these materials influence their applications as biosensors and biomedical devices (Figure 1). Whilst the applications of 2D materials for biotechnology are extensively reviewed, the goal of this review is to highlight and discuss the importance of dimensionality and its impact to the properties that exhibited. Using recent biosensing and biomedical examples, we discuss, from a material science perspective, and demonstrate how 2D materials have improved and enhanced research in this field. A summary of recent applications in biosensors and selected biomedical applications, including antibacterial, antifouling, tissue engineering and drug delivery, are presented in table 1 and table 2, respectively. In regard to bio-applications, we briefly discuss the main characteristics of 2D materials and their surface effects that are important to the biosensors and biomedical field – namely surface area, electrochemical properties, and functionalization - and have facilitated their research and development.

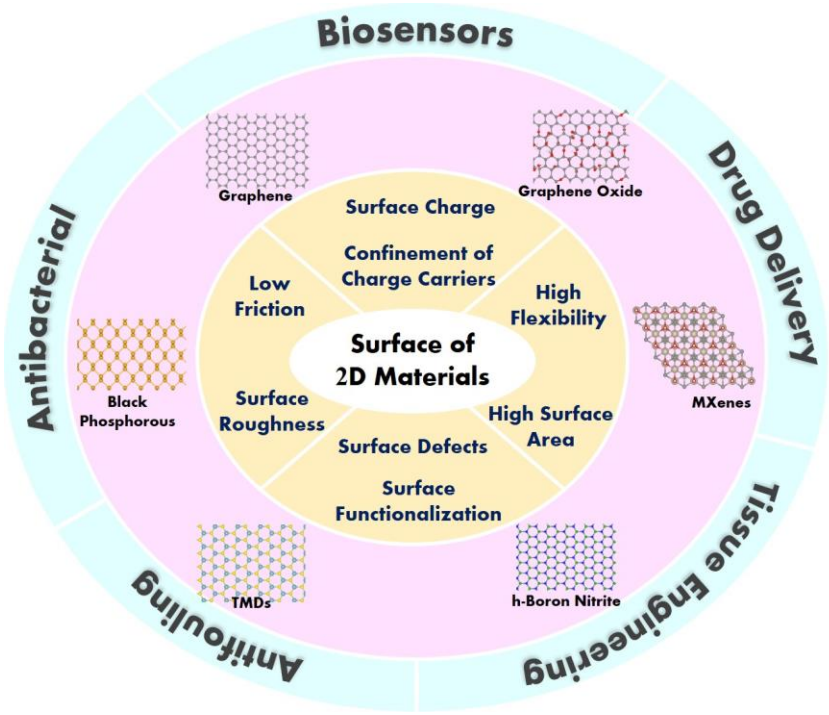

Figure 1. Summary of the surface properties of two-dimensional materials (2D) and their main biomedical applications.

Table 1. Surface properties effects of 2D materials in recent biosensing applications. Common properties such as high surface area, biocompatibility, excellent mechanical strength and flexibility etc. are omitted to negate repetition.

2D Material	Surface Properties	Application on Biosensors	Target	LOD/ LR	Reference
Graphene and its derivatives	Zero gap semiconductor, excellent conductor, high electron transfer capabilities, ease of functionalization and doping, fluorescence quenching	FET (rGO)	Brain natriuretic peptide (BNP) in whole blood	100 fM	[13]
		Optical (graphdiyne)	DNA	25 fM	[14]
		Optical GO	Glutathione	4 nm/ 0.02-20 µM	[15]
		PEC (GO)	PSA	0.3 $pg.mL^{-1}$/ 1 $pg.mL^{-1}$–100 $ng.mL^{-1}$	[16]
		EC (rGO)	Acetylcholine	4 nm/ 4 nm-800 µM	[17]
		EC (rGO)	Glucose nonenzymatic	0.3 µM/ 0.0025-0.1525 mM	[18]
	Semiconducting, tunable band gap (~1.8 eV monolayer), high on/off ratios, photoluminescence, ease of functionalisation *via*	Optical	Intracellular caspase-3 activity	0.33 $ng.mL^{-1}$ / 2-360 $ng.mL^{-1}$	[19]
		SPR	BSA	14.5 nM	[20]
		PEC	Acetamiprid	16.7 fM/ 0.05 pM–1 nM	[21]
		SPR	E Coli	94 $CFU.mL^{-1}$	[22]

2H MoS_2	thiol and amide chemistry, fluorescence quenching capabilities, catalytic abilities (can act as nanozyme)	SPR	miRNA-141	0.5 fM	[23]
		FET	Prostate cancer biomarkers	100 $fg.mL^{-1}$	[24]
		EC	miRNA-21	0.78 fm (DPV) 0.45 fM (EIS)/ 10 fM-1 nM	[25]
		EC	miRNA-21	0.26 pM/ 1 pM-10 nM	[26]
		EC	Cancer cells	50 $cells.mL^{-1}$/ 50-106 $cells.mL^{-1}$	[27]
2H WS_2	Semiconducting, tunable band gap (~2.05 eV monolayer), photoluminescence, ease of functionalization, fluorescence quenching capabilities	SERS	Cardiac marker myoglobin	0.5 aM / 0.5 aM-5 pM	[28]
		PEC	DNA	2.29 fM/ 5 fM-50 pM	[29]
		PEC	Human Epididymis Protein 4	0.03 $pg.mL^{-1}$/ 0.1 $pg.mL^{-1}$-10 $ng.mL^{-1}$	[30]
		EC	Trichloroacetic acid (TCA) and $NaNO_2$	0.4 $mmol.L^{-1}$ (TCA) 0.2 $mmol.L^{-1}$ ($NaNO_2$)	[31]
		EC	Carbohydrate antigen 72e4 (CA72-4)	0.6 $U.^{L-1}$/ 2-50 $U.L^{-1}$	[32]
BP	Semiconducting,	EC	TCA, $NaNO_2$ and H_2O_2	1.0 $mmol.L^{-1}$ (TCA), 0.033 $mmol.L^{-1}$ ($NaNO_2$) and 0.67 $mmol.L^{-1}$ (H_2O_2)	[33]

	direct and tunable band gap (~1.88 eV monolayer) high carrier mobility, moderate on/off ratios, broad absorption range	FETs	IgG	0.065–3.25 nM	[34]
MnO_2	semiconducting, exhibits nanozyme activities, broad spectrum quencher	Colorimetric assays nanozyme	Glutathione	300 nM	[35]
g-C_3N_4	Semiconducting, large band tunable band gap (~2.75eV monolayer) photosensitivity and activity, capability to convert light into electricity, emits strong fluorescence (λ=~440 nm)	ECL	DNA	3.6×10^{-14} M/ 10 μM–0.1 fM	[36]
Ti_3C_2 MXenes	Metallic, excellent conductivity, ease of functionalization, hydrophilic surface	EC	Cancer biomarkers (carcinoembryonic antigen (CE))	0.000018 $ng.mL^{-2}$ / 0.0001–2000 $ng.mL^{-1}$	[37]
Heterostructures					
FTO/PDDA/g-C_3N_4/MoS_2/CdS QDs	Co-sensitization due to coupling of 2D materials, accelerate electron transfer, broaden wavelength range of absorbed light, enhanced	PEC	DNA	0.32 pm/ 1 pM–2 mM	[38]

	photoelectricity				
MoS_2/graphene aerogel	Framework increases surface area, improved charge transfer and conductivity	EC	Glucose	0.29 mM/ 2-20 mM	[39]
ZnO nanosheets grown on 2D thin-layered MoS_2	Surface electrostatic forces enabled growth of ZnO on MoS_2, low surface roughness, enhanced surface affinity for negatively charged DNA, increased electron transfer	EC	DNA	6.6×10^{-16} M	[40]
Gold nanoparticles (AuNPs) with hybrid 2D materials consisting of boron nitride (BN) and tungsten disulphide (WS_2)	Improved charge transfer at the interface, introduction of new electronic states leading to enhanced performances	EC	H_2O_2	3.0 mM/ 0.15-15.0 mM	[41]
Molybdenum trioxide (MoO_3) anchored onto the reduced graphene oxide (RGO)	Improved electron shuttling leading to faster transfer rates and efficient heterogeneous electron activity	FET	Breast cancer biomarker human epidermal growth factor receptor-2 (HER-2)	$0.001 ng.ml^{-1}$/ 0.001-500 $ng.mL^{-1}$	[42]

* EC: Electrochemical; ECL: electrochemiluminescence; FET: Field Effect Transistors; PEC: Photoelectrochemical; SPR: Surface Plasmon Resonance

Table 2. Surface properties effects of 2D materials in antibacterial, antifouling, tissue engineering and drug delivery applications. Common properties, such as high surface area and biocompatibility are omitted to negate repetition.

2D Material	Surface Properties	Effect	Efficiency	Reference
2H MoS_2	The high negative surface charge; Semiconducting; Low friction; Low surface roughness	Antifouling	Antifouling layer against natural organic matter and *E. coli*	[43]
1T MoS_2 1T $MoSe_2$ 1T WS_2	The high negative surface charge; Metallic; "Nanoknives"	Antibacterial	Antibacterial properties against Gram-negative bacteria Escherichia coli	[44]
2H WS_2	The high negative surface charge; High surface area; Semiconducting; "Nanoknives"	Antibacterial	Antibacterial properties against *S. aureus* and *E. coli* with antibacterial rates of 91.3% and 89.7 %, respectively.	[45]
BP	The high negative surface charge; High surface area; Semiconducting; Photocatalytic; "Nanoknives"	Antibacterial	Antibacterial properties against *E. coli and B. subtilis* with 91.65% and 99.69% of efficiency respectively	[46]
			Antibacterial properties against *E. coli* and *S. aureus*	[47]

			under irradiation (808 nm laser, 1 W cm^{-2})	
GO	The high negative surface charge; Smooth surface; Semiconducting; "Nanoknives"	Antibacterial	Inhibition of *S. aureus* and *E. coli.*	[48]
GO and Nano GO	Irregular surface (wrinkles); "Nanoknives"; Photothermic	Antibacterial	Antibacterial properties against gram-positive *S. aureus* and gram-negative *E. coli* bacteria under irradiation of ultra-low doses (65 mW cm^{-2}) of 630 nm light	[49]
GO/ZnO Nanocomposite	The high negative surface charge; Oxygen functional groups; "Nanoknives"	Antibacterial and Biofilm inhibition	Inhibition of biofilm formation around 90% *Escherichia coli, Salmonella typhi, Pseudomonas aeruginosa* and *Shigella flexneri*	[50]
Graphene/Chitosan Nanocomposites	Irregular surface (wrinkles); "Nanoknives"	Antibiofilm	Inhibition of biofilm formation Pseudomonas aeruginosa and Klebsiella pneumoniae in 94 and 92 %, respectively	[51]
GO/Alginate nanocomposite bioinks	High surface roughness; Oxygen functional groups; Negative charge;	Tissue Engineering	Enhanced osteogenic differentiation by the 3D scaffolds printed with the bioink based on mesenchymal stem cells (MSCs) and alginate/GO	[52]
GO/ silk fibroin (SF)/ nano-hydroxyapatite (nHAp) nanocomposite			CO/SF/nHAp scaffold with high capability for stimulating bone marrow mesenchymal stem cells (BMSCs) adhesion and proliferation.	[53]
GO/BP/ poly(propylene fumarate nanocomposite	High surface roughness; Oxygen functional groups;	Tissue Engineering	3D printed BP/GO/ poly(propylene fumarate) Scaffolds enhance cell proliferation, osteogenesis and mineralization process	[54]

	Phosphate groups			
MXenes- $Ti_3C_2T_z$ - poly(lactic acid) (PLA) nanocomposite	High surface roughness; High hydrophilicity; High binding energy between their surfaces and bridging Ca^{2+} ions	Tissue Engineering	Enhanced the in vitro adhesion, proliferation, and osteogenic differentiation of MC3T3-E1 mouse preosteoblasts	[55]
hBN-gelatin nancomposite	Lewis "acid behaviour" due the vacant "p" orbital of the B atom on h-BN	Tissue Engineering	The hBN-gelatin nancomposite fibers with high bioactivity to form bonelike hydroxyapatite; High biocompatibility in human bone cells (HOS osteosarcoma cell line)	[56]
hBN - Poly(propylene fumarate) (PPF) nanocomposite	High surface roughness; Thermal conductivity		Enhanced mechanical strength and adsorption of collagen I protein, improved the extracellular matrix (ECM) deposition, cell attachment and spreading for bone grafts	[57]
rGO	Hydrophobic surface; □-□ stacking interactions at the surface	Drug Delivery/ Chemotherapy	Delivery Doxorubicin (DOX) with a maximal loading rate of 98% at pH 9	[58]
Hyaluronic acid-decorated GO nanosheet	Coexistence of hydrophobic and hydrophilic surface properties; π–π stacking interactions and hydrogen bonding at	Drug Delivery/ Photothermal therapy (PTT)/ Chemotherapy	DOX delivery release rate of 45% in 16 h. Antitumor efficiency due to photothermally controlled and redox-triggered cytoplasmic rapid delivery of DOX molecules, with the combined chemo- and photothermal therapy	[59]

GO - based molecularly imprinted polymer (MIP)	the surface; good water dispersion; strong near infrared (NIR) absorption	Drug Delivery	Specific recognition to carcino-embryonic (CEA) tumor markers, biocompatibility, and pH sensitivity for DOX delivery.	[60]
hBN - assembled with adenine	π–π stacking interactions; porosity; thermal conductivity	Drug Delivery/ Chemotherapy	High DOX loading capacity (up to 36.2%) by tuning the pH and temperature	[61]
MoS_2 modified with hyaluronic acid	Thermal conductivity; high near-infrared absorption	Drug Delivery/ Chemotherapy/ PTT	Delivery of melanin and DOX; Photothermal conversion efficiency of the 55.3%	[62]
MXenes-Ti_3C_2	Thermal conductivity, free electrons, negative surface charge	Drug Delivery Photothermal/ Photodynamic/ Chemotherapy	Delivery DOX with a high loading capacity of 84.2% and stimuli responsive DOX releasing performance upon pH-responsive and NIR laser.	[63]
BP	Thermal conductivity, high near-infrared absorption.	Drug Delivery Photothermal/ /Chemotherapy	Delivery of Fluoxetine by irradiation of NIR light (808 nm); Fluoxetine loading capacity onto BP of 700%; Released capacity of 90% of Fluoxetine with NIR for 30 min	[64]
BP- mesoporous silica nanoparticles (MSNs)			Thrombolytic drug release under (NIR) laser irradiation (808 nm, 0.2 W cm^{-2}). Loading efficiency of 92.78%.	[65]

2. Surfaces and reduction of dimensionality

Every 3D material is made up of a bulk, that contains the majority of the atoms, and a surface, where its atoms come in contact and interact with the external and surrounding environments. By its very definition, 2D materials are *all* surface, as all its atoms are the surface itself, and there is no bulk. While on a macro scale this may be a drawback and can seem weak (similar to comparing a piece of paper to a thick plank of wood), interestingly on the nanoscale, the reduction of dimensionality reveals several unique properties that broadens their use and applications.[8,10] In regards to biosensing and biomedical applications, here we discuss some of the unique properties that arise from reducing the dimensionality and how they can be applied or is beneficial for biosensing and biomedical applications such as: antibacterial activity, antifouling, tissue engineering and improvement of the biocompatibility. Although the methods for obtaining these 2D materials and fabrication of the devices have a very important role in the overall properties, we will only briefly discuss these topics and processes in this short review as there are several recent reviews dedicated to these topics.[66–69]

2.1 - Surface area and removal of van der Waals interactions

The first, and most obvious advantage of decreasing the dimensionality, is the increase of surface area and, by extension, increase in the surface area-to-volume ratio.[70,71] This is a very important characteristic as the higher the amount of exposed surface area, the better (and more) the reactant can have accessible contact with the material. Moreover, by having a planar structure, 2D materials have unprecedented levels of sensitivity to the surrounding environments and changes to its properties due to chemical or biological interactions are not lost in the bulk response. Besides that, the high surface area of the 2D materials permit the higher density immobilization of bioreceptors, such as enzymes, antibodies, DNAs and/or aptamers, onto surface of the 2D materials, improving the sensitivity of biosensors based on these materials. Electrical biosensors based on 2D materials, such as chemiresistors and field effect transistors (FETs, discussed later) take advantage of this property.[2,72] For example, Bazylewski et al.[73] recently describes a solid state chemiresistor based on cysteine modified MoS_2 for the rapid (within a second) sensing of cadmium ions in drinking water in the sub-ppb range (1-10 ppb, figure 2(a)). The sensor also exhibited excellent selectivity towards cadmium as there was negligible interference from the other heavy metals.

Within a monolayer of 2D material, the bonds that hold the atoms together are very strong. The nearby in-plane atoms are covalently bonded with low defects density and thus give rise to superior mechanical properties.[74] For example, graphene, which is reported be the stiffest 2D material with the

highest Young's modulus of ~1 TPa[75–77], has a tensile strength that is 1000 times stronger than its bulk counterpart, graphite, and is 100 times stronger than steel. Yet even with their high mechanical resistance, due to the atomic thickness of the 2D crystal, 2D materials show exceptional flexibility and are ideal candidates for next generation flexible electronics, which could be used in wearable health-monitoring devices, biocompatible electronic skins and implantable biomedical devices, such as biosensors and prosthesis (discussed later).[78,79]

While mono and few layer 2D materials offer numerous advantages as aforementioned, the stacking and combination of different 2D materials together also has its own merits and broadens the use and potential applications of 2D materials. Within the class of 2D materials, there are many types of materials with unique electronic structures ranging from conducting to insulating. As such, there are many possibilities for creating layer-by-layer solids, known as 2D or van der Waals heterostructures, that can have unique and synergistic properties.[80–82]

The stability and stacking of the layers is achieved through weak van der Waals interactions at the interface of each 2D monolayer. However, as these interactions are relatively weak, the intrinsic properties of the individual layers are still maintained or present with other intriguing properties that are not observed in the single 2D material nor it´s bulk.[83,84]Although the use of the heterostructure format is primarily for energy harvesting and storage, within recent years, there has been growing interest in its implementation for biosensing, in particular for photoelectrochemical biosensing (see electrochemical section).[85,86]

2.2 - Confinement of electrons

As aforementioned, another fascinating and important aspect of 2D materials, upon reduction of its dimensionality, is the rise of unique electronic and optical properties that are not typically observed in the bulk. The manifestation of these properties can be attributed to the confinement of electrons into a 2D plane.[87] Several popular 2D materials and their properties are summarized in table 1 and 2. This is a highly interesting aspect to 2D materials, and there are many recent reviews that describe the emergence of these properties and discuss them in detail.[88,89]

Briefly, in materials, the electronic and optical properties are dictated by its electronic band structure, which describes the electron movement through the material. Upon reducing the dimensionality, the periodicity in the direction perpendicular to the 2D plane is removed and results in large changes to the band structure and the electronic and optical properties that are expressed.[90] These modified band structures are responsible for the many unique properties found in 2D materials, such as

the high conductivity in graphene and the photoluminescence of monolayer MoS_2. Moreover, as the band structures dictate the properties, modifying and tuning of the band structures also allows for tailoring the properties for specific applications and outcomes. In particular to biosensing, applications such as FETs and electrochemical based sensors can benefit greatly as on/off current ratios can be modulated and improve or facilitate faster electron transfers; thus, leading to more sensitive biosensors.[91] Tuning of the band structure can be achieved by various approaches, including electrical, mechanical and chemical means.[92,93]

2.3 - Defects and functionalization

In its bulk 3D form, the material layers are weakly held together by van der Waals interactions that can be easily broken by applying an external force, such as mechanical or shear stress.[8,94,95] This approach is known as the top-down approach, as it starts with a bulk piece as the source of the 2D materials, and includes exfoliation methods such as sonication assisted exfoliation, lithium intercalation exfoliation and, the now famous, scotch-tape method. The other approach, known as the bottoms-up approach, is to start with a substrate where the 2D material will be assembled from chemical precursors under specific conditions - typically high temperatures and pressures. While each approach has its merits, there are various limitations that arise and must be addressed depending on the desired application or outcomes.

While there are many reports that study and define the influences of various factors and reaction parameters during the synthetic process,[96–98] a key issue that presents itself in both approaches is the pristiness of the resulting 2D material, in particular for applications that require monolayers. In top-down approaches, the exfoliation is unpredictable and can result in 2D material of various layers (i.e. monolayers, bi-layers, bulk etc.), structures (i.e. nanosheets, nanoflowers, quantum dots etc.) and surface defects and vacancies. Similarly, the bottoms-up approach can also produce 2D materials with surface/atomic vacancies and replacement of atoms in the crystal lattice (doping). Fortunately, whilst these defects can severely affect the properties, these defects can also be used to fine tune the properties or to give the 2D material additional functionalities.[99]

Perfection is not always everything, and this can be particularly true for 2D materials. Whilst pristine crystalline materials are necessary for electronics, the presence of defects have been shown to change or enhance the physical and electrochemical properties, and great efforts have gone into investigating and harnessing these effects for better and faster applications.[99–101]

Surface vacancies, where an atom is missing from the crystal lattice, are often the result of the violent nature of exfoliation methods, such as ion intercalation, or intentionally created by various means, such as irradiation. For example, point defects in graphene, such as the absence of carbon atoms (either/both sp_2 or sp_3) can lead to changes in the electronic sp_2 structure and effect the chemical reactivity on the surface.[102] Chen et al.[103] recently reported a systematic evaluation of the electronic structure of MoS_2 with lattice defects. Here, by purposefully creating sulphur vacancies on CVD grown MoS_2, the authors found that the ´defective´ samples had faster hydrogen evolution kinetics in comparison to pristine samples. This increase in activity can be attributed to the formation of new catalytic/active sites in the basal plane.[104,105] Moreover, the authors also examined the effects of various substrates, such as gold, graphene and h-BN, and found that the electronic energy levels were influenced by the charge transfer at the interface.

Doping is an effective approach to increase the catalytic or electronic properties of 2D material. In particular, doping with other metals can introduce strains and defects to the basal plane and, ultimately, increase the density of active sites, and thus the electrocatalytic activity and rate of charge transfer.[92] Harnessing the effects of both metal atom doping and defective sites, Ramaraj et al.[106] developed a new electrocatalyst for biosensing using manganese (Mn) doped $MoSe_2$ via a hydrothermal synthetic process (figure 2(b)). By introducing Mn into the crystal structure, the authors observed the creation of Se vacancies[107] that led to increased catalytic and electronic activity. Moreover, the vacancies were also used as active sites for the effective immobilization of enzymes, which in their case was myoglobin. The modified 2D material was then evaluated by EIS for hydrogen peroxide sensing with reported ultralow detection limit of 0.004 μM and sensitivity of 222.78 $\mu A/\mu M/cm^2$. This work not only demonstrates the advantages of doping, but also the additional benefit of surface vacancies.

In regards to biosensors, and other applications that may require selectivity, selectivity is a primary concern that should be considered. As the selectivity is highly influenced by the nature of the 2D materials and the target analyte, approaches to integrating and modifying the surface of the sensing material are the most effective ways to fine tune the sensor itself. In particular, the interactions of 2D materials and the target molecule follows two distinctive mechanisms: chemisorption and physisorption.[2,108]

Chemisorption is when there are covalent interactions between the surface of the 2D material and other molecules, such as the target analyte or ion. This is a common approach to tailor the properties of 2D materials, as the electronic band structure can be modulated.[95] In the scope of bio-applications, defect sites can be used as anchoring points for chemical functionalization of molecules to enhance

selectivity.[109,110] This approach is typically adopted for biosensing, where receptor molecules are employed for their specific recognition capabilities to target analytes. Moreover, by functionalizing and increasing the amount of analyte-surface binding sites, the electronic properties of the material can be modulated or tailored to improve the sensitivity and lower the limit of detection. [3,111,112] A recent example was demonstrated by Vulcano et al.[113] who compared the sensing capabilities of electrochemically exfoliated GO with and without surface functionalisation. The surface of the GO was covalently functionalized with dopamine, using NHS/EDAC as a linker, to target NADH (figure 2(c)). Due to the presence of dopamine, which introduced 1,2-dihydroxyphenyl moieties to the surface, the sensitivity of the modified GO showed enhanced sensitivities towards NADH by 180% and improved limit of detection. Furthermore, they concluded that the performance improvement could also be attributed to the increased chemical stability of the electrode and measurements.

Chu et al.[114] reports the covalent functionalization of MoS_2 with a diazonium salt that preserved the semiconducting properties (figure 2(d)). However, interestingly, the author´s DFT studies suggested that only a single surface vacancy was required to render the entire MoS_2 surface functionalizable. The authors describe this effect as similar to the ´cooperative effect´, as seen with bioploymers such as proteins and nucleic acids, where the covalent interactions between molecules or surfaces are strengthened upon binding events with other molecules. The authors then extend their technique to covalently tether active green fluorescent protein and mCherry to the MoS_2 surface, demonstrating the use of this approach for bioimaging and biosensing. By examining the fluorescence images, it was revealed that the dyes had attached only to the areas where the MoS_2 was functionalized, and that the fluorescence was increased when both dyes were used together.

Physisorption occurs when other molecules and ions interact with the surface of the 2D material without any covalent bonding. These interactions typically occur due to the reactivity, and compatibility, of the functional groups on the molecule to the surface of the 2D material, such as hydrogen bonding, electrostatic forces, pi–pi interactions, cation - pi, etc. For example, molecules are able to physisorb onto the basal planes of MoS_2 due to interactions between the molecule and the surface through van der Waals forces.[115] Moreover, the electronic characteristics of pi-pi systems, such as aromatic molecules, has been shown to have influences that are able to modify the electronic and optical properties of 2D materials.[116,117]

For applications that follow the physisorption mechanism, the sensors typically have rapid response times and fast recoveries, as there is no chemical reaction required to attach and detach the analyte to the electrode/surface of the 2D material. Some studies have achieved higher adsorption of

molecules onto the sensor surface by inducing the defect sites on the surface of the 2D material.[118–120] Recently, Ma et al.[121] compared the use of defective and pristine graphene as a gas sensor for NO_2 at room temperature (figure 2(e)). The response of the defective graphene based sensor towards 100 ppm NO_2 was 13 times higher than that of the pristine graphene sensor, and also showed excellent selectivity, reproducibility and stability. The authors found that by tuning the defect density and size, via ion irradiation and H_2 etching, more adsorption sites were created and, thus, improved the performance of the sensor.

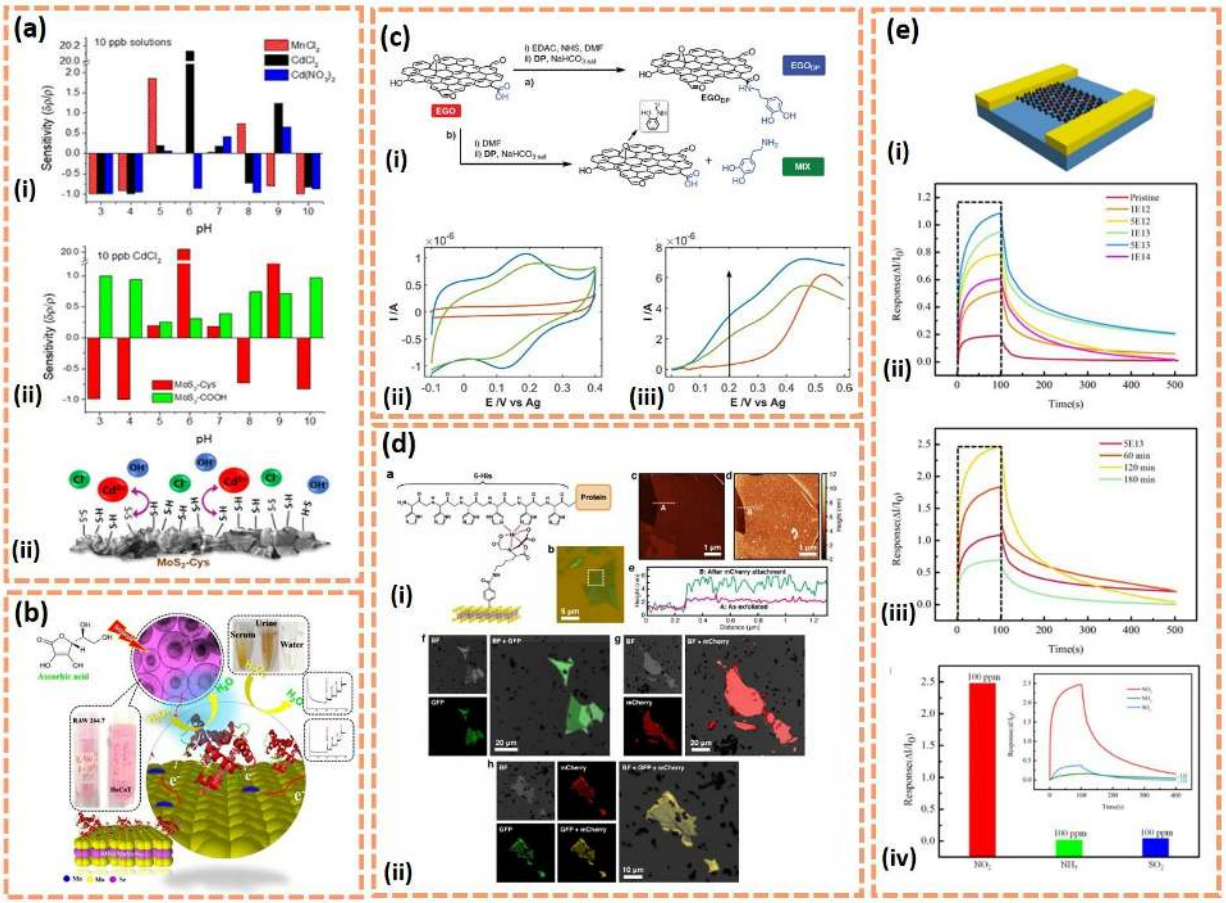

Figure 2: (a) Bar graphs demonstrating the sensitivity of (i) MoS_2–Cys sensors to different metal ions depending on the pH and metal ion used and (ii) MoS_2–COOH compared to MoS_2–Cys using a 10 ppb solution at varying pH, and (ii) charge transfer at the nanostructured surface of MoS_2–Cys films (Adapted with permission from ref (73). Copyright (2020) American Chemical Society, further permission related to the material excerpted should be directed to the ACS). (b) Schematic illustration of real-sample analysis (Adapted with permission from ref (106). Copyright (2019) American Chemical Society). (c) (i) Synthetic route to EGODP (path a) and to MIX (path b), (ii) CVs recorded at EGO (red line), EGODP (blue line) and MIX (green line) modified-SPEs in 0.1 M PBS (pH 7.0) and 0.1 M KCl after 20 potential cycles, and (iii) voltammetric traces recorded at the same modified electrodes after addition of 0.5 mM NADH; only the forward scan after subtraction of the relevant signal obtained in the absence of NADH is reported (Adapted with permission from ref (113), Copyright 2018 © IOP Publishing. Reproduced with permission. All rights reserved.). (d) (i) Attachment of active proteins to MoS_2 with optical and AFM images of the

pristine and modified material with mCherry after functionalization and (ii) bright field, confocal fluorescence microscopy images in GFP (green) and mCherry (red) channels, and fluorescence images overlaid onto BF images, after protein attachment process (Adapted with permission from ref (114). Copyright 2018 American Chemical Society). (e) (i) schematic of the defective graphene (DGr) based sensor with the response to 100 ppm NO_2 for varying (ii) irradiation influence and (iii) H_2 etching time at room temperature and (iv) comparison of responses of the DGr-based gas sensor to different gases at room temperature (Adapted with permission from ref (121), licensed under a Creative Commons Attribution (CC BY) license, Copyright 2019 AIP Publishing).

3. Recent biosensing and biomedical applications

As discussed, 2D materials are very well-suited for biosensing and biomedical applications and offer many advantages. In this section, we highlight a few of the more recent studies of 2D material based bio-applications, and we discuss how these applications have harnessed the 2D planar structure and the unique properties for more reliable or enhanced operations. In particular, we focus on the common uses of 2D materials for biosensing, which includes electrochemical, field effect transistors (FETs) and optical methods, and the more recent biomedical technologies, such as antibacterial and antifouling applications, drug delivery and tissue engineering. For clarity, we organize this section on the basis of the applications and discuss the properties and types of 2D materials which are typically used in the field.

3.1 - Biosensing

The unique and versatile properties of 2D materials offer great advantages for biosensing applications. In many of these cases, the 2D material is used as the sensing element (working electrode) to enhance the detection signal upon interaction with the analyte or to facilitate charge transfer. Moreover, in this regard, recent biosensing trends have also implemented 2D materials in many on/off biosensing platforms, due to their conducting or semiconducting properties, and also as fluorescence quenchers in optical systems.

3.1.1 - Electrochemical

On a commercial level, electrochemical biosensors are currently the most widely available and have been developed to integrate and target various bioanalytes, such as enzymes/enzymatic reactions, nucleic acids, antibodies etc.[122] and have been adopted in various formats, including field-effect transistor (FET)[123], electrochemical impedance/amperometric sensors,[124,125] and photoelectrochemical sensors.[126] Typically, the sensing principle of electrochemical biosensors is to convert the interaction between the recognition element and analyte into an electric signal. These interaction events are electron charge transfer processes that occur at the electrode surface; thus the electrode material has great effects on the performance of the sensor.[127,128]

Nanostructures and nanomaterials, like 2D materials, have facilitated considerable progress in biosensor research and development. The surface of 2D materials are ideal substrates for the development of electrochemical biosensors, due to their large specific surface area, outstanding electrical properties, and excellent biocompatibility[90,129,130] . These characteristics create a favorable microenvironment for the immobilization of bioreceptors on the surface of these 2D materials, conferring selectivity to these electrochemical sensors. Moreover, by integrating 2D materials and harnessing their unique properties, performance parameters, such as the sensitivity and selectivity, can be greatly enhanced.[131] In this regard, for electrochemical sensing, 2D materials with high conductivities, such as graphene and reduced graphene oxide, are typically employed to increase the charge transfer and conductivity of the electrode surface, and consequently increase its sensitivity. In fact, the use of graphene and its derivatives are widely examined and numerous studies have demonstrated that by coupling functional graphene and electrochemical methods, the overpotential was effectively decreased, while the current response was greatly enhanced.[132] On the other hand, 2D materials with semiconducting properties, such as several MXenes and the transitional dichalcogenides, have also been widely explored for electrochemical sensing due to their surface properties and tunable intrinsic band-gaps. Wang and Zhu et al[133]. took advantage of the surface properties of the MXene-Ti_3C_2 to fabricate a mediator-free electrochemical biosensor to detect hydrogen peroxide (H_2O_2). The hemoglobin (Hb) was encapsulated onto the MXene-Ti_3C_2 layers by the use of nafion and the biosensors exhibited good performance for the amperometric detection of H_2O_2 with a wide linear range of 0.1–260 μM, as well as an extremely low detection limit of 20 nM. The surface of the MXene-Ti_3C_2 provided a favorable microenvironment for Hb to undergo a facile electron-transfer reaction, in this way contributing to the excellent sensitivity of this biosensor to detect H_2O_2. In addition to the high surface area, Kim et al.[134] also took advantage of the flexibility of 2D materials and developed a flexible electrochemical biosensor based on MoS_2 for the detection of three endocrine hormones in real serum samples (figure 3(a)). By adopting a competitive assay and enzyme reaction mechanism, the novel biosensor displayed high sensitivity and reproducibility that were comparable to standard immunoassay equipment. Thus further demonstrating the versatility of 2D materials for electrochemical biosensing.

Recently, a typical trend that is seen with 2D materials, is the pairing of the 2D material with other 2D materials. Since the first demonstration of 2D materials as biosensors, many have discovered that there are numerous factors that influence the performance of the sensor and that each material suffers from its own drawbacks. However, due to the surface nature of the 2D material, it is quite easy and facile to combine various materials together to synergistically enhance the material and the sensor.

For example, it is widely reported that MoS_2 exemplifies great catalytic activities due to the exposed edges,[70,135] but often suffers from low electrical conductivities and a tendency to stack or

agglomerate, which decreases the amount of accessible surface area[136] and affects electrochemical performance. In a synergistic approach, Yang et al.[137] electrodeposited ZnO nanosheets onto ultrasonicated exfoliated MoS_2 scaffold for the electrochemical detection of DNA (figure 3(b)). The negatively charged MoS_2 nucleated and supported the growth of the ZnO through electrostatic interactions, while the presence of the positively charged ZnO improved the capacity of the nanocomposite for DNA immobilization and improved the electrochemical performance and an ultralow detection limit of 6.6×10^{-16} M was obtained. In another example, Jeong et al. demonstrates the synergistic effects of 2D MoS_2 and graphene in an aerogel for glucose detection.[136] In addition to harnessing the catalytic ability of MoS_2, the 3D aerogel structure increased the surface area, which allowed for higher amounts and better immobilization of glucose oxidase, while the continuous graphene based framework exhibited superior conductive properties when compared to 2D MoS_2/rGO. Using flow-injection amperometric analysis, their MoS_2/graphene aerogel glucose sensor had rapid response times of 4 s, sensitivity of 3.36 lA/mM, LOD of 0.29 mM and a linear detection range between 2-20 mM.

Photoelectrochemical (PEC) biosensing and bioanalytics are becoming increasingly popular within recent years, and has even created its own subclass of innovative research. In comparison to conventional electrochemical and optical methods, the main attraction of this method of sensing can be attributed to the remarkable sensitivities and reduced background signals that can be achieved due to the total separation of the different energy forms of the excitation source (light) and the detection signal (electricity). Furthermore, the instrumentation of PEC is simpler, more cost effective and easier to miniaturize in comparison with optical techniques, which typically require additional apparatus that are often more complicated and expensive.[138,139]

As the PEC detection signal mainly stems from the photoelectric conversion capabilities of the photoactive material, the choice of electrode material is thus critical to the overall performance. Due to the optoelectronic properties and surface nature of 2D materials, 2D materials are ideal candidates for construction of PEC biosensors, in particular 2D heterostructures. Specially, the semiconducting 2D materials are ideal for PEC platforms due to their light absorbing capabilities, conduction and valence band positions and tunable band gaps, and flexibility as planar structures. In this regard, TMDs, such as MoS_2 and WS_2, and graphitic carbon nitride (g-C_3N_4) have been widely explored for PEC biosensing. Wang et al.[140] proposes a novel PEC biosensor for ultrasensitive detection of miRNA-396a based on a MoS_2/g-C_3N_4/TiO_2 heterojunction decorated with antibody functionalized AuNP for signal amplification (figure 3(c)). The developed biosensor had a low detection limit of 0.13 fM and a linear range of 0.5-5000 fM. The authors attributed e high sensitivity of the sensor to the staggered matching of the electronic band

structures of the MoS_2/g-C_3N_4/TiO_2 heterojunction, which increased the charge carrier concentrations when irradiated.

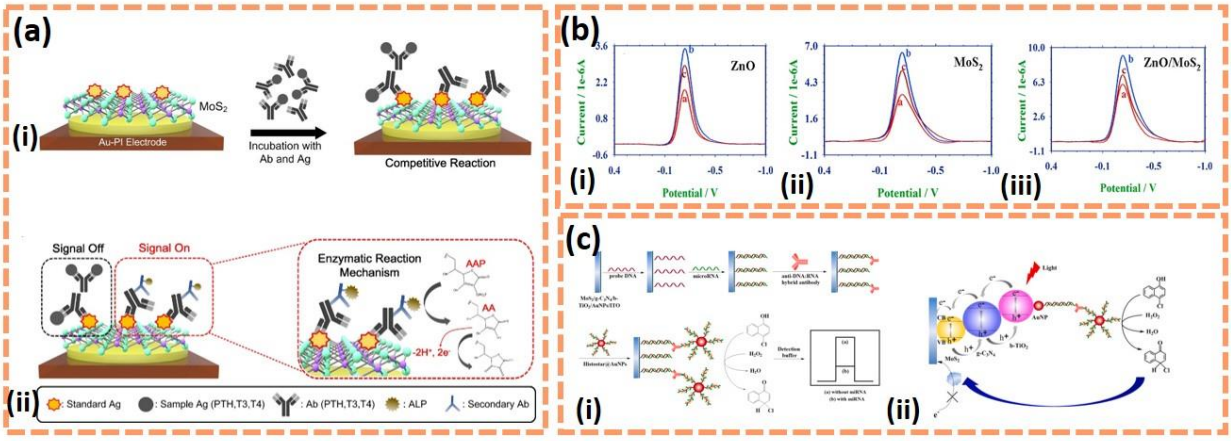

Figure 3: (a) Process of Competitive Assay and Enzymatic Reaction Mechanism for PTH, T3, and T4 Antigens (Immune Complexes): (i) immobilization of standard antigens (Ag) and competitive reaction between sample antigens and the antigen-conjugated surface of MoS_2 on a flexible Au–PI electrode with corresponding antibodies (Ab) and (ii) signal on/off by competitive reaction with the enzymatic reaction mechanism.(reprinted (adapted) with permission from ref (134), Copyright 2020 American Chemical Society) (b) Comparison DPVs of 2.0×10^{-5} M myoglobin with (i) ZnO, (ii) MoS_2 and (iii) ZnO/MoS_2 modified electrodes with and without ssDNA and dsDNA (Adapted with permission from ref (137). Copyright 2018 Elsvier). (c) (i) schematic illustration of the biosensor construction process and (ii) the photocurrent generation mechanism of the PEC biosensor (Adapted with permission from ref (140). Copyright 2019 Elsevier).

3.1.2 - Field-effect transistors (FETs)

Biosensors based on field-effect transistors (FETs) are highly attractive as they promise real-time label-free electrical detection, scalability, inexpensive mass production, miniaturization, the use of low volume of sample, and the possibility of on-chip integration of both sensor and measurement systems[141]. 2D semiconductor materials, such as graphene, TMDs and black phosphorus (BP), have attracted significant interests for the development of highly sensitive biosensors based on FETs devices[22], replacing the traditional silicon technology[142]. It is due to the outstanding properties of these materials such as the high charge carrier mobilities (μ) ($\mu_{graphene}$ = 15 000 cm^2 V^{-1} s^{-1}, $_{BP}$ ~ 1000 cm^2 V^{-1} s^{-1} and the acceptable $\mu_{2H\ MoS2}$ ~ 60 cm^2 V^{-1} s^{-1}), high flexibility, biocompatibility, large specific surface area and facile chemical functionalization [22]. In addition, a monolayer of graphene allows all carbon atoms to be exposed to the surroundings, in this way the carbon atoms can directly interact with the analyte, leading to increased sensitivity.

A typical FET biosensor based on 2D materials for evaluating liquid samples consists of a 2D material layer (the semiconductor channel), deposited on top of an insulator substrate, between two metal electrodes, called by the source (S) and drain (D). A third electrode, the gate electrode (usually a reference microelectrode, Pt wire or Ag/AgCl), is immersed in an electrolyte solution, where the 2D semiconductor material is exposed. The current between the S and D electrodes (Ids) could be modulated by an electric field generated by the gate voltage (Vgs), due to change of the 2D material carrier densities [143,144]. Upon interaction of an analyte on the 2D material surface, even at low concentrations, the values of the conductance, represented by the Ids current change significantly.

FETs biosensors based on 2D materials draw attention due to their impressive sensitivity. This feature is highlighted in the recent work of Seo et al.[145]. The authors developed a graphene FET (GraFET) biosensor for the label free detection of the SARS-CoV-2 in clinical samples without any sample treatment step. For this, the authors immobilized a specific antibody against SARS-CoV-2 spike protein on the graphene surface through the non-covalent functionalization with the 1-pyrenebutanoic acid succinimidyl ester (PBASE), by the pi-pi interactions between the graphene surface and pyrene group of PBASE (Figure 4 (a (i)). The GraFET biosensors were able to detect the SARS-CoV-2 spike protein at concentrations of 100 fg/ml in the clinical transport medium used in the nasopharyngeal swab (Figure 4 (a (ii)). In addition, the GraFETs biosensors successfully detected the SARS-CoV-2 in clinical samples from patients with a LOD: $2.42x10^2$ copies/ml (Figure 4 (a (iii)).

The sensitivity of FET-based biosensors is not only related to the semiconductor material used as a channel, but also with the ionic concentration of the solution containing the analyte[146]. One of the major hurdles to lower the detection limit of FET- based biosensor is shielding of the molecule charge by the counter ions in solution (termed Debye shielding). Outside the Debye length (the length of the electrical double layer (EDL)), which is <1 nm in physiological solutions, the charges are electrically screened. An increase in the Debye length can result in reduced screening effect and allow for a more sensitive electrical detection of charged biomolecules [147,148]. Hwang et al.[148] were pioneers in exploring the deformation of the graphene surface, by curving or bending it, to improve the sensitivity of the GraFETs biosensors for detection of nucleic acids (DNA and/or RNA). The enhancement could be attributed to the modulation of the Debye length (or volume) and by the induced band-gap opening in the graphene channels due to strain. The probe DNA anchored via a linker molecule on flat and crumpled graphene channels of the FET biosensors was affected in different ways by the Debye length. The flat graphene has a constant Debye length; whilst in the crumpled graphene, the Debye length oscillated at the peaks and the valleys of the crumpled surface (Figure 4 (b (i)). The surface of crumpled graphene was disorganized with herringbone-like structures (Figure 4 (b (ii)) and these structures contributed to the disorganization in

the distribution of the counter-ions of the EDL over a longer distance away from the surface of the crumpled graphene. This accounted for decreases in the screening effect for the crumpled graphene in relation to the flat graphene (Figure 4 (b (iii)). The theory proposed by the authors was fundamental from the results obtained by the density functional theory (DFT) and molecular dynamics (MD) simulations, and by the expressive results in the determination of miRNA spiked in PBS buffer and undiluted human serum samples in a concentration of 600 zM and 20 aM, respectively, when compared to the negative control testes (Figure 4 (b(iv)). In this way it is clear that the shape, deformation and roughness of the surface of the 2D materials also have an important role in the sensitivity of the FETs biosensors.

Other 2D materials such as 2H-MoS_2 (semiconductor phase) and BP have been explored in the development of FETs biosensors (table 1). The FETs biosensors based on 2H MoS_2 exhibit an advantage over the GraFETs that is the high current on/off ratio ($I_{on/off}$), that can exceed 1 x 10^8, which is much higher than that of GraFETs biosensors[22,149]. As monolayer 2H MoS_2 is a semiconductor with a direct band gap of 1.8 eV, this offers a much higher gate-tunable conductance for the 2H MoS_2 FETs in relation to graphene, that has a band gap of 0 eV and due this low $I_{on/off}$ values and in some conditions, leakage current, that can impact in the sensitivity of these devices[22,150].

The few-layer BP was demonstrated interesting characteristics for the development of FETs devices, as a p-type semiconducting material with mobility up to 984 cm^2 V^{-1} s^{-1} (10 nm sample) and a direct band gap that is tunable from 0.3 eV for bulk BP to 2.0 eV for monolayer BP[151]. However, the biggest challenge that needs to be overcome to use BPFETs as biosensors is the poor chemical stability of this material in the presence of the oxygen and water. BP can degrade quickly to oxygenated phosphorus (POx), which makes biosensing processes on its surface unfeasible[22].

For use the BPFET as a biosensor, Chen et al.[34] passivated the surface of the BP with a thin film of Al_2O_3, as a dielectric layer, to protect the BP from the oxidation process and to immobilize gold nanoparticles labelled antihuman IgG antibody onto Al_2O_3, for the label free detection of IgG antigens. The BPFET biosensor exhibited a low LOD of ~10 $ngmL^{-1}$ due the electrical properties of the BP and the amplification signal of the gold nanoparticles. However, many efforts still need to be made in order to develop strategies for stabilizing the surface of BP in aqueous environments and allowing for exploration of the real potential of BPFETs as biosensors.

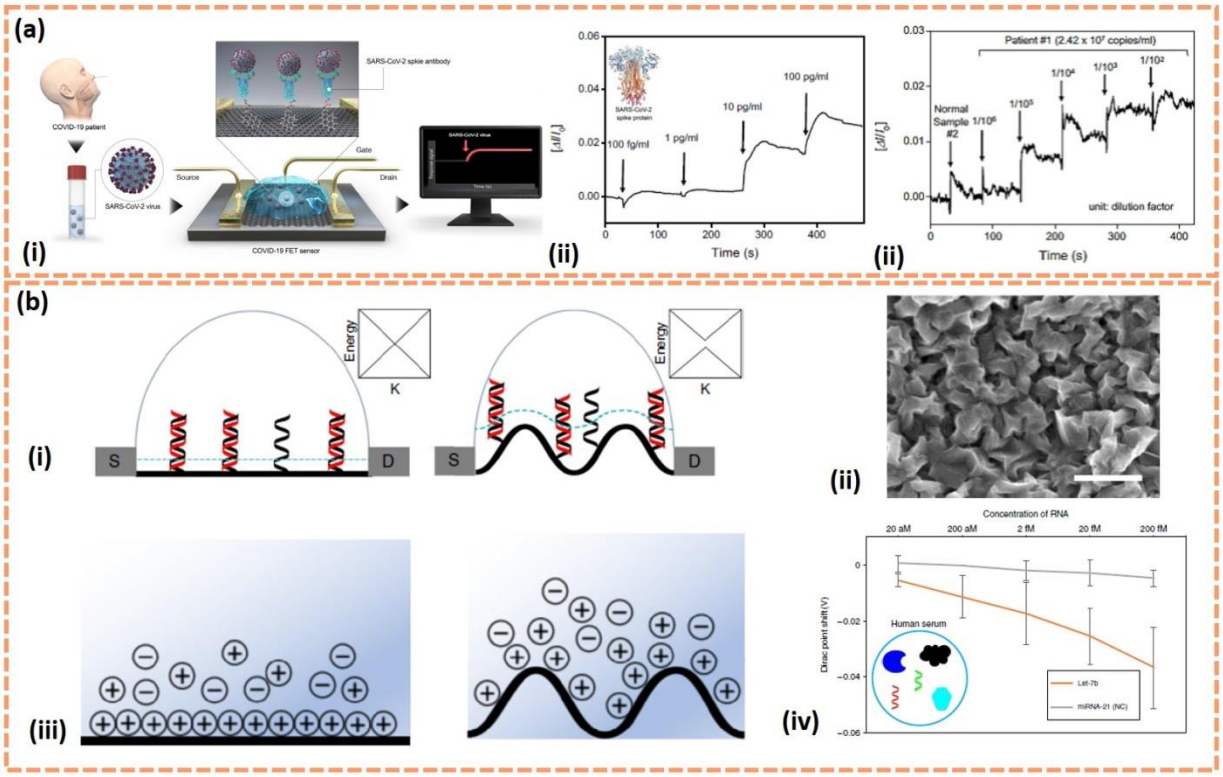

Figure 4. (a) Graphene-based field effect transistors biosensors for COVID19 diagnosis. (i) Schematic diagram of COVID-19 FET sensor operation procedure. Graphene as a sensing material is selected and SARS-CoV-2 spike antibody is conjugated onto the graphene sheet via 1-pyrenebutyric acid n-hydroxysuccinimide ester, which is an interfacing molecular as a probe linker. (ii) Real-time response of COVID- 19 FET toward SARS-CoV-2 antigen protein in UTM, insert the SARS-CoV-2 spike protein. (iii) Real time response of COVID-19 FET toward SARS-CoV-2 virus from clinical sample (Reproduced with permission from Ref. (145). Copyright 2020 American Chemical Society). (b) Scheme and characterization of flat and crumpled graphene FET biosensor. (i) Cross-sectional scheme of the flat (left) and crumpled (right) graphene FET DNA sensor. Probe (black) and target (red) DNA strands are immobilized on the surface of graphene. The blue dot lines represent Debye length in the ionic solution and the length is increased at the convex region of the crumpled graphene, thus more area DNA is inside the Debye length, which makes the crumpled graphene more electrically susceptible to the negative charge of DNA. The inset boxes represent qualitative energy diagram in K-space. Graphene does not have an intrinsic bandgap. However, crumpled graphene may open the bandgap. (ii) SEM images of crumpled graphene. The scale bar is 500 nm (iii) ELD structures of flat (left) and crumpled graphene (right). Loosely structured EDL of crumpled graphene leads to the smaller capacitance value (ref). Nucleic acids absorption and hybridization test on flat and crumpled FET. (iv) Dirac voltage shift of the FET sensor with miRNA detection of hybridization. Target RNA spiked in human serum was treated on the FET sensor (Adapted with permission from Ref (148). Copyright 2020Springer Nature).

3.1.3 - Optical

By exhibiting tunable optoelectronic properties, 2D materials are also ideal materials for optical sensors. Their unique optical and vibrational characteristics, such as photoluminescence, enhanced

photoelectron interactions and plasmonic behaviors, has facilitated the construction of high performance biosensors with remarkable sensitivities and ultrafast response times that rival, and can potential surpass or replace, the use of current electrical biosensors.[152,153,154] Typically, 2D based optical sensors will employ the 2D material as a substrate, due to the planar structure and high surface area and aforementioned properties, rather than an optical label. In particular, the TMDs pose as ideal candidates for optical based sensing due to its tunable band gaps and abilities to absorb in the visible and NIR ranges upon doping.[155] The most common 2D material based optical sensors include surface plasmon resonance (SPR), surface-enhanced Raman spectroscopy (SERS) and fluorescence based sensors.

Both SPR and SERS methods offer outstanding sensitives and the capability of single molecule and label free detection. Considered as a standard biophysical tool[156], surface plasmon resonance (SPR) sensors have found increasing bio-applications, ranging from environmental monitoring to healthcare diagnostics.[157] There are many advantages of SPR sensors, including rapid analysis, high specificity and dynamic measurements, amongst many others. Using an emerging 2D material, atimonene, Xue et al.[158] developed an SPR biosensor for ultrasensitive detection of miRNA (figure 5(a)). Despite possessing similar lattice structure to graphene, the author´s DFT studies revealed that antionmene exhibits strong spin-orbit coupling and has greater interaction with ssDNA due to the higher delocalized 5s/5p orbitals. Motivated by this, the authors then obtained 2D atimonene nanosheets by liquid phase exfoliation and coated it onto a gold film for SPR sensing. To add selectivity to the antimonene, probe DNA conjugated gold nanorods were adsorbed onto the surface. Using miRNA-21 and miRNA-155, the ultralow detection limit of 10 aM was obtained, surpassing current sensing methods, and a concentration-dependent response up to 10^{-11} M.

SERS has also emerged as a powerful and reliable technique for bio and chemical sensing and analysis. The integration of 2D materials for SERS is typically focused to enhance the Raman signal by increasing the charge transfer rate between the (sensor) surface and the adsorbed analyte. In particular, TMDs exhibit excellent charge transfer properties[159] and SERS activities when coupled to plasmonic gold or silver nanoparticles.[160,161] Due to its compatible work function, WS_2 has been shown to provide better SERS enhancement than MoS_2; the most widely studied transitional metal dichalcogenide[162]. Motivated by this, Shorie et al.[163] developed a SERS based aptasensor for the label free detection of myoglobin using a WS_2-AuNP nanohybrid (figure 5(b)). The in-situ coupling of WS_2 and AuNP together greatly enhanced the SERS platform both chemically and electromagnetically, while the specific aptamers increased the selectivity. The sensor displayed enhanced sensitivity, as low limit of detection of 0.5 aM was obtained, and great selectivity for myoglobin whilst in the presence of hemoglobin and bovine serum albumin.

Although SPR and SERS biosensors have achieved exceptional results, these platforms are not always user friendly as specific instruments and setups are required. Consequently, naked-eye detection methods are potential solutions as they are easy to use and, additionally, can be adapted for point of care (POC) devices. The most common use of 2D materials is in fluorescence based biosensors, where the exceptional intrinsic fluorescence-quenching abilities of 2D materials are harnessed. In particular, for microfluidic and on/off sensors,[164] fluorescence based biosensors typically employs the Förster resonance energy transfer (FRET) approach that pairs a fluorophore (fluorescent donor) and a quencher (light absorbing acceptor) to obtain a signal.[165,166] Yang et al.[167] demonstrates the FRET approach for multiplexed sensing of lectins and bacteria with a fluorescence array that uses saccharide functionalized multi-colored QDs and 4-mercaptophenylboronic acid (PBA) functionalized MoS_2 nanosheets (figure 5(c)). In their array, through chemical interaction of the saccharides and PBA, the QDs are initially absorbed onto the MoS_2 and the fluorescence is quenched. Then, depending on the lectins that are present/added, the QDs begin to detach from the MoS_2 surface, thereby restoring the fluorescence. This effect was attributed to the diverse affinities of the lectins to the saccharides, which causes competitive binding of the lectins to the QDs, and leads to desorption from the MoS_2 surface. In the presence of multiple lectins, a distinct fluorescence response pattern was observed and analyzed with linear discriminant analysis. The authors concluded that there was 100% accuracy in identification between multiple lectins and bacteria reaching detection limits as low as 3.7 nM and 66 cfu/mL, respectively.

In another example, Zamora-Galvez et al.[168] use a similar approach for naked-eye detection of immunoglobulin G (IgG) in a paper-based lateral flow immunoassay (figure 5(d)). Here, the authors use CdSe QDs modified with anti-human IgG functionalized as the fluorescence probe, graphene oxide nanosheets as the quencher and SiO_2 beads as a spacer. The SiO_2 beads are functionalized with the detection antibodies that capture the analyte and flow towards the test and control lines *via* capillary action. Upon reaching the test line, the analyte forms an immunosandwich with the QDs and the (pre-attached) SiO_2. The GO is then added to the paper strip as the ´revealing´ agent. The presence of the SiO_2 bead creates enough distance between the QD and the GO that hinders quenching of the fluorescence. Whereas, without the analyte and the spacer bead, the fluorescence can be easily quenched as the GO comes in direct contact with the QDs.

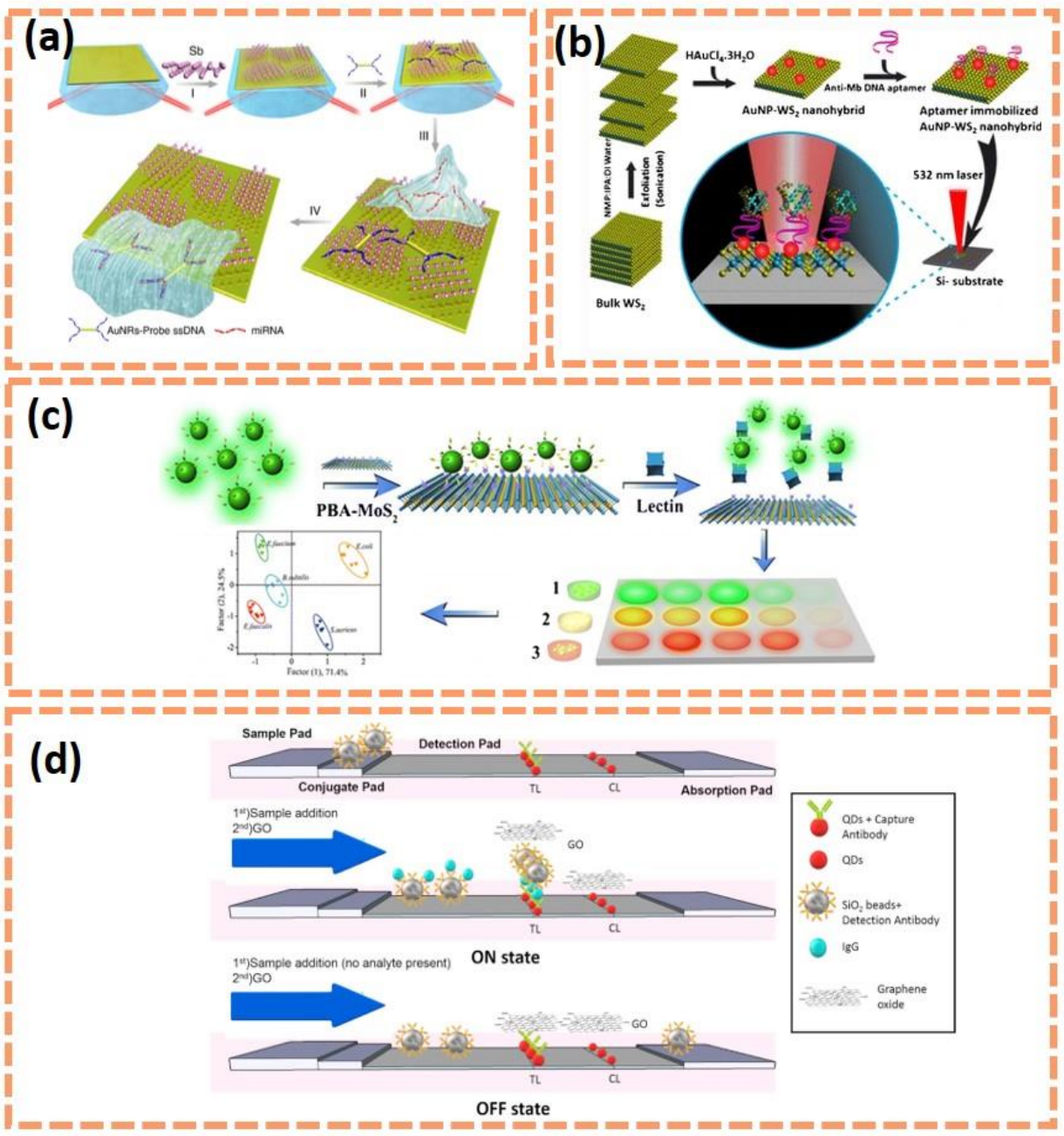

Figure 5: (a) Fabrication of a miRNA sensor integrated with antimonene nanomaterials. Schematic illustration of the strategy employed to detect antimonene-miRNA hybridization events (reproduced with permission from ref (158). Copyright 2019 Nature). (b) Schematic showing stepwise synthesis and fabrication of Au-WS_2 nanohybrid based SERS active platform (reproduced with permission from ref (162). Copyright 2018 Springer). (c) Schematic illustration of the design rationale for lectin detection (reproduced with permission from ref (167). Copyright 2018 Springer). (d) Scheme of the developed lateral flow (reproduced with permission from ref (168). Copyright 2018 Elsvier).

3.2 - Biomedical

The 2D materials are receiving increased interests in biomedical applications owing to their special physicochemical and surface properties. In this section, we will focus on the recent application of 2D material for antibacterial, antifouling, tissue engineering and drug delivery. A widely studied approach is the use of 2D materials for optical biomedical applications, such as bioimaging, photothermal therapy and theranostics. While the surface area and number of layers has great influence on the optical properties of 2D materials, these optical biomedical applications will not be thoroughly discussed in this review; as their applications rely more on the intrinsic optical properties than on the surface of the 2D material. However, great progress has been made in this field of biomedical research and there are many recent reviews that brilliantly discuss these achievements.[169–172]

3.2.1- Antibacterial

2D materials have attracted considerable attention in biomedical applications due to their antimicrobial activity[173–175]. The antimicrobial activities of the 2D materials, such as graphene materials (GMs, defined by graphene and its derivatives such as GO and rGO), MoS_2, h-BN, BP and some MXenes, are related with the physicochemical and structural characteristics of these materials. So, in this way, the surface properties of these materials play an important role, as all the interaction between the 2D materials and these pathogens, mainly bacteria, occur at their surface.

The first materials that had their antimicrobial activities investigated were the GMs in 2010[176]. Since then, several mechanisms have been proposed to explain how these materials display antimicrobial activities. However, the main three most accepted mechanisms are: i) nanoknives derived from the action of sharp edges; ii) oxidative stress mediated with the production of reactive oxygen species (ROS), and iii) wrapping or trapping of bacterial membranes derived from the flexible thin-film structure of GMs [177,178]. Other recent mechanisms have been proposed as the extraction of lipid bilayers[179] , the interference of protein−protein Interactions (PPIs)[180] and the “self-killing” effect[181]. The Figure 6(a) summarize the main mechanisms of the antimicrobial activities of GMs.

The nanoknives mechanism is related with the extremely sharp boundaries of the GMs nanosheets. The blade like GMs nanosheets can cause physical damage to the membranes of microbes and leakage of the intracellular matrix, thus leading to inactivation of the microorganisms [177,178]. In this way, the control of the number of layers (exfoliation degree) in the GMs is a crucial factor for the antimicrobial activity by this mechanism, as the number of layers can increase the thickness of the GM nanosheets, thus decreasing the effectiveness of the nanoknives effect.

The oxidative stress mechanism can be attributed to the capacity of the GMs nanosheets to induce the oxidative stress in bacteria. The oxidative stress can interfere with bacterial metabolism and disrupt essential cellular functions, leading to cellular inactivation or even cell death[177,178]. The GMs nanosheets are able to mediate the generation of ROS (such as hydrogen peroxide (H_2O_2), superoxide anions ($O_2^{\bullet-}$), hydroxyl radicals ($OH^{\bullet}$), or singlet molecular oxygen) by the adsorption of O_2 on the defect sites and edges of the GMs nanosheets[182]. In this way, the density of functional oxygen groups and defects on the surface of the GMs nanosheets contribute to the high generation of ROS and explain the excellent antimicrobial activity of the GO[176,183–185].

The last, and most acceptable, mechanism for the antimicrobial activity of GMs is related with wrapping or trapping effects in the bacterial membranes. GMs nanosheets can entrap the bacteria or microorganisms and isolate them from their surroundings, making them incapable to proliferate due to gas exchange and access to nutrients, leading to bacterial growth inactivation or bacterial death[183,186].

Other graphene-like nanomaterials also possess enormous potential in antibacterial applications, displaying antimicrobial mechanisms similar to that of GMs[47,174,187,188]. The emerging class of the 2D MXenes have also attracted attention for their intrinsic antibacterial properties. Rasool et al [189] reported the antibacterial properties of micrometer-thick titanium carbide ($Ti_3C_2T_x$) MXene membranes against *Escherichia coli (E. coli)* and *Bacillus subtilis (B. ubtilis)* bacteria. The $Ti_3C_2T_x$ MXene membranes were prepared by vacuum filtration of a colloidal solution of single- and few layers of $Ti_3C_2T_x$ (Figure 6 (b (i-ii)). The antibacterial rate of fresh $Ti_3C_2T_x$ MXene membranes reached more than 73% against *B. subtilis* and 67% against *E. coli* as compared with that of control PVDF, while aged $Ti_3C_2T_x$ membrane (after 30 days storage) showed over 99% growth inhibition of both bacteria under the same conditions (Figure 6 (b (iii)). The authors attributed the antimicrobial effectiveness of the $Ti_3C_2T_x$ MXene membranes to the sharp edges of the nanosheets, which caused physical damage and disruption of the bacteria cellular membranes, inducing oxidative stress that can be generate by the anatase TiO_2 nanocrystals (produced from the natural oxidation of the $Ti_3C_2T_x$ in air). Moreover, the negatively charged and hydrophilic surface of the $Ti_3C_2T_x$ nanosheets may have also facilitated the inactivation of the bacteria by direct contact interaction with its surface.

MoS_2 nanosheets have also been explored for antimicrobial applications based on the oxidative stress and the nanoknives mechanism[174,190,191]. The conductivity of the MoS_2 nanosheets also play an important role in its antimicrobial properties. Due to the higher electric conductivity of the metallic phase, 1T MoS_2 has been shown to present with higher antimicrobial activity than that of the semiconducting 2H MoS_2. The higher conductivities can render lower electrical resistance for electron transfer from bacterial

intracellular components to the external environment, promoting the oxidative stress of the bacteria[192]. Another important factor of the antimicrobial activity of the MoS_2 is the shape of the nanomaterial. Recently, Xu et al.[191] evaluated this parameter by comparing MoS_2 nanosheets and nanoflowers against *S. aureus* and *E. coli* (Figure 6 (c (i-ii)). For this they obtained the MoS_2 nanosheets and nanoflowers from the galvanostatic electrolysis in a Mo electrode, by tuning the current in the system. The MoS_2-nanoflowers showed relatively improved antibacterial performance in relation to the MoS_2 nanosheets. The higher surface area of the MoS_2-nanoflowers was attributed to cause more oxidation stress to bacteria upon contact than the nanosheets (Figure 6 (c (i-ii)).

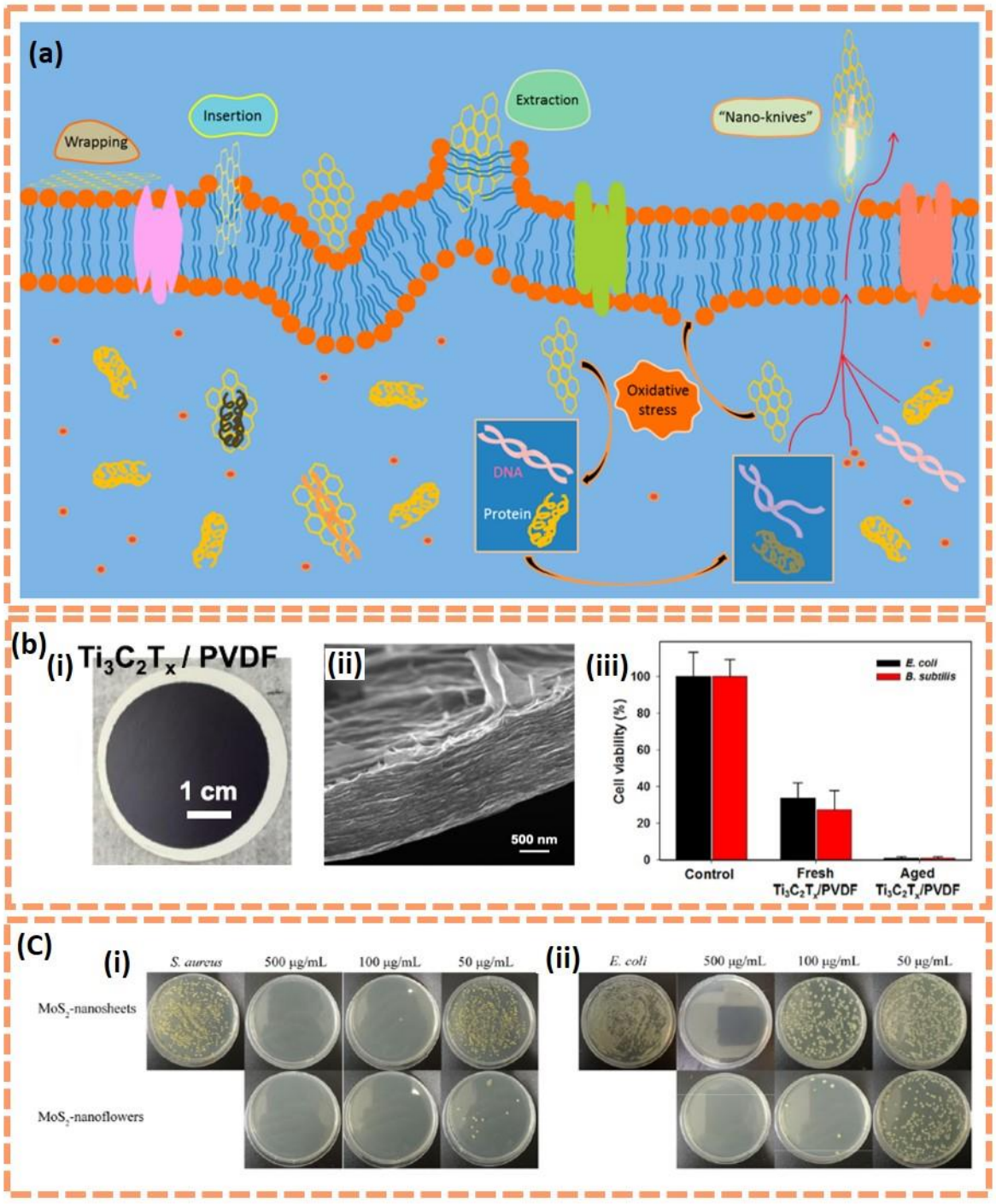

Figure 6. Antimicrobial properties of the 2D Materials. (a) Mechanisms of the antimicrobial activities of GMs (Reproduced with permission from ref (177). Copyright 2016 American Chemical Society). (b) Antibacterial membrane based on 2D $Ti_3C_2T_x$ (MXene) nanosheets. (i) $Ti_3C_2T_x$ (MXene) membrane on a PVDF support and (ii) its cross-sectional SEM image. (iii) Cell viability measurements of *E. coli* and *B. subtilis* grown on fresh and aged $Ti_3C_2T_x$ (MXene) membranes for 24 h (Adapted from ref (189), Copyright 2017 Springer Nature). (c) The effect of the shape of the MoS_2 nanosheets on their antibacterial properties. (i) The optical images of *S. aureus*, (ii) *E. coli* incubated 4 h with MoS_2 nanomaterials of different concentration (Adapted with permission from ref (191). Copyright 2020 Elsevier).

3.2.2 - Antifouling

The formation of biofilms by microorganisms around implantable medical devices still represents a challenge for the biomedical community. Surfaces that are in direct contact with biological fluids, such as a catheter and urinary probe, are an ideal environment for bacteria to adhere and proliferate, leading to infection in the patients[193]. Similarly, surfaces of membranes for nanofiltration processes also suffer from the formation of biofilms, which reduces their performance and deactivates their surface. The best strategy to combat this is based on the use of biomaterials on the surface of these biomedical implantable devices and membranes that can repel the microbes or kill them in the surrounding areas [193,194]. In this scenario the use of 2D materials as a coating, composites, or membrane among others, emerges as an interesting approach for antifouling application, due their unique surface properties.

In particular, 2D materials with high surface hydrophilicity and negative charge stand out. By controlling the biofouling via an anti-adhesion mode, unfavorable conditions for natural organic matter (NOM) and some bacteria are created and hinder their growth onto the surface. In addition, the surface roughness of 2D materials also plays an important role in the antifouling properties, where several authors have shown that the surface roughness increases the adhesion forces resulting in larger bacterial attachment to rougher surfaces[195,196]. In this case, MoS_2 presents special features as extremely low friction and low surface roughness and, along with GO, have been explored for this purpose[43,80]. Alam et al.[43] performed a comparative study between the antifouling properties of MoS_2 and GO. Both materials present a highly negative zeta potential in deionized water, -41.33 ± 0.5 mV and -40.34 ± 0.76 mV for GO and MoS_2 respectively. However, the contact angle measurements of the GO and MoS_2 were 25 ± 5.4 and 42 ± 4.6, respectively, suggesting that GO was slightly more hydrophilic than MoS_2. But, on the other hand, MoS_2 exhibited slightly better antifouling properties than GO. In most cases, the deposition of NOM and *E. coli* (which are Gram-negative bacteria and are strongly negatively charge) was significantly lower on MoS_2 than GO due to the presence of functional groups on GO, which bound more easily with the foulants, and the low roughness of the MoS_2 surface.

Another interesting approach to further improve the antifouling properties of 2D materials is the preparation of nanocomposites and hybrid nanomaterials with metal and oxide nanoparticles and polymers, among others, that exhibit antibacterial properties[197,198]. Graphene and GO have been explored in the development nanocomposite with improved antifouling properties and the recent work of Maruthupandy et al.[51] showed impressive anti-biofilm formation activities of a graphene/chitosan nanocomposite against biofilm producing *P. aeruginosa* and *K. pneumoniae*. The formation of biofilm by

Pseudomonas aeruginosa and *Klebsiella pneumoniae* was inhibited at 94 and 92 %, respectively, by the use of only 40µg/mL of the graphene/chitosan (GR/CS) nanocomposite in PBS. The effectiveness of the GR/CS nanocomposite in hindering the biofilm formation was attributed to causing disruptions to the biofilm aggregation via membrane damage and distorting cellular morphology.

3.2.3 Tissue engineering

Bodily tissues can be easily damaged by physical trauma, infection, or tumors. Many efforts have been dedicated to treat and repair various tissues, mainly in bone and dental tissue regeneration. In this scenario, the integration of 2D materials in the tissue engineering approach appears as an advantageous alternative[199]. Besides the outstanding physical and chemical properties of the 2D materials, these materials possess also excellent biocompatibility, biodegradability, surface functionality, high mechanical resistance and plasticity, that render these materials as suitable applications in tissue engineering as coatings, nanocomposites, among many others [200]. Specifically, the surface properties of the 2D materials play an important role in tissue engineering, mainly due the interaction between the 2D material and the tissues - that is an interfacial phenomenon. The unique large surface area and surface chemical properties of the 2D materials are strongly related with their biocompatibility, which is the key parameter to consider if a material is a biomaterial. The excellent mechanical strength and low cellular toxicity of 2D materials improve much more the biocompatibility of scaffolds and promotes osteogenic differentiation, and is beneficial to bone tissue engineering[201]. Besides that, the antimicrobial and antifouling properties of several 2D materials, as previously discussed, are very interesting for applications in wound repair[202] and in medical implants, helping in the prevention of bacterial biofilm formation on the implantable medical devices.

The successful use of the 2D materials as a coating for implantable biomedical devices is also related with the surface topography of these materials and plays a crucial role in the regulation of the cellular behavior[200]. In this scenario, graphene and its derivatives like GO and rGO, stand out as these materials have distinctive topographical characteristics, such as wrinkles and ripples etc., that can increase the surface roughness of the substrates[199,200,203]. The rough surface of graphene and its derivatives provide anchorage sites for cells, that allows the cells to easily adhere to the substrates. Moreover, the oxygen functional groups of GO (carboxyl, hydroxyl and epoxide groups) are able to adsorb serum protein in culture medium, by attaching to molecules or surfaces, and promote the cellular differentiation and growth[204]. This is evidenced in the use of a substrate recovered with GO film to promote the differentiation of dental pulp stem cells (DPSCs)[205]. Besides that, the negatively charged GO surface can promote electrostatic interactions with the positively charged calcium phosphate (due to the calcium

moieties), enabling the development of nanocomposites based on GO and calcium phosphate and to induce the osteogenesis process on bone regeneration applications[206,207].

One recent example of the development of a nanocomposite based on GO for bone regeneration, is the work performed by Li and collaborators[208]. The authors developed a bioactive three-dimensional GO foam (GF)/polydimethylsiloxane (PDMS) /zinc silicate (ZN) scaffold with enhanced osteoinductivity properties for bone regeneration. The nanocomposite was synthesized via dip coating and hydrothermal synthesis processes, resulting in the interconnected macroporous structure (Figure 7 (a)). The authors combined the properties of all the materials, such as: i) the 3D structures of the GO foam, to improve the proliferation of mouse bone marrow mesenchymal stem cells (mBMSCs) and play an active role in osteogenic differentiation in bone tissue engineering; ii) the flexible stiffness and biocompatibility of the PDMS, that can increase the mechanical properties of the GF scaffold without changing its good cell compatibility and iii) the zinc silicate particles, to provide zinc and silicon ions to the GF scaffold to improve the ability of stem cells to survive and differentiate into bones; to achieve scaffolds exhibiting a porous characteristic with organic−inorganic components similar to natural bone tissue. The nanocomposite scaffold displayed excellent biocompatibility and the ability to induce mBMSC proliferation and preferential osteogenic differentiation. The in vivo analysis of critical bone defects in rabbits demonstrated superior bone formation in defect sites in the GF/PDMS/ZS scaffold group at 12 weeks of post implantation without any significant inflammatory response (Figure 7 (a (i-xii)).

Another 2D material that has been attracting attention in bone tissue engineering is BP[209,210]. Besides having all the unique properties of the 2D materials, BP has a special feature, that is related with its chemical composition - the phosphorus atoms. As previously mentioned in this review, the BP has poor chemical stability in the environments with oxygen and water and rapidly degrades to oxygenated phosphorus (POx), releasing phosphate ions. However, the phosphate ions are a major constituent of bone minerals and play an important role in bone regeneration[211]. Based on that, Huang et al.[212] proposed to develop a 3D hydrogel based on BP nanosheets (BPNs) to consistently and mildly provide phosphorus ions to accelerate bone regeneration without introducing foreign calcium. The 3D hydrogel was fabricated by photo-crosslinking of gelatin methacrylamide, BPNs, and cationic arginine-based unsaturated poly(ester amide)s. The incorporation of the BPNs in the 3D hydrogel scaffolds improved the mechanical performance of the hydrogels and promoted the capture of the calcium ions to accelerate the biomineralization process in defected bone (Figure 7(b)).

Besides the graphene, and BP many other 2D materials, and nanocomposites based on these materials have been explored in tissue engineering, where their surface properties confer these materials outstanding performance when incorporated into scaffolds, as can be seen in the table 2.

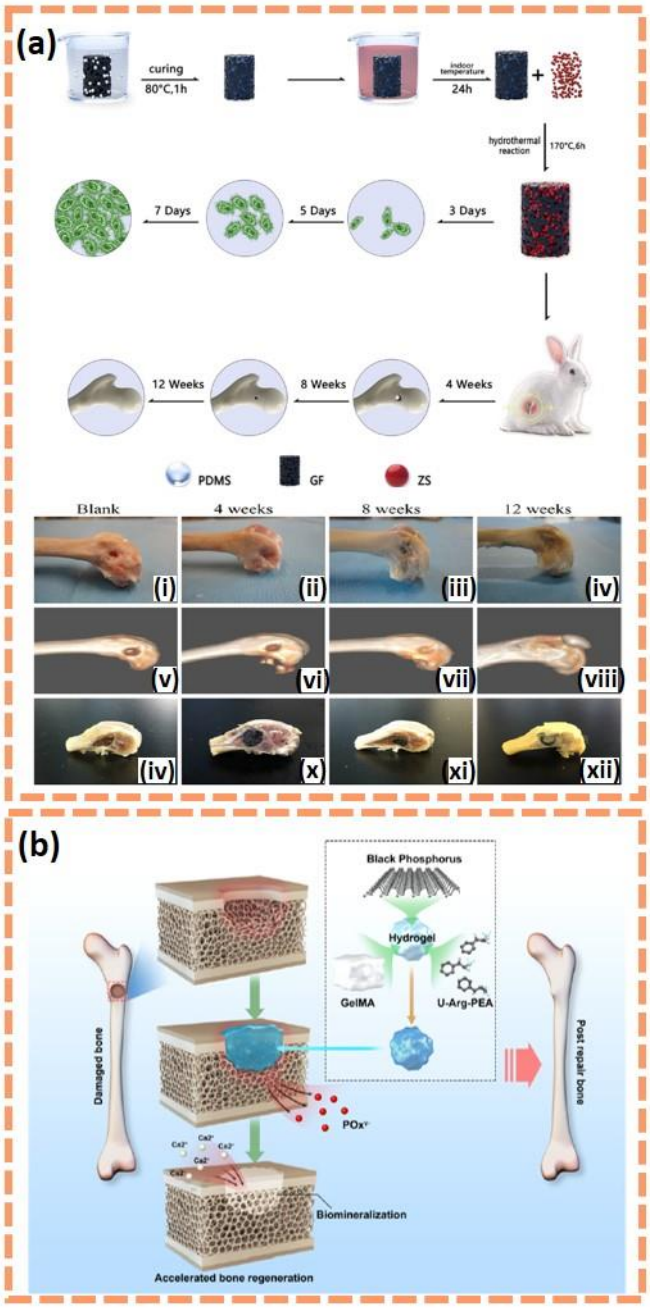

Figure 7. The application of 2D materials for bone tissue engineering. (a) Schematic illustration of the synthesis of nanocomposite based on three-dimensional GO foam (GF)/polydimethylsiloxane (PDMS) /zinc silicate (ZN) scaffolds and their potential application in osteoblast differentiation. A 6 mm × 10 mm rabbit bone defected in vivo and the gross anatomy of the (i) blank group at 12 week post-surgery and (ii-iv) GF/PDMS/ZS composite scaffold group at 4, 8, and 12 weeks after surgery, respectively. 3D CT reconstruction model diagram of the (x) blank group

at 12 weeks after surgery and (vi-viii) GF/PDMS/ZS composite scaffold group at 4, 8, and 12 weeks after surgery, respectively. Sagittal plane anatomy of the (ix) blank group at 12 weeks after surgery and (x−xii) GF/PDMS/ZS composite scaffold group at 4, 8, and 12 weeks after surgery, respectively (Adapted with permission from ref (208). Copyright 2019 American Chemical Society). (b) Schematic illustration of the preparation of black phosphorus nanosheets based 3D hydrogel platform via photopolymerization of gelatin methacrylamide (GelMA) and cationic arginine-based unsaturated poly(ester amide)s [U-Arg-PEAs], for effective bone regeneration. (Reproduced with permission from ref (212). Copyright 2019 American Chemical Society).

3.2.4 – Drug Delivery

Drug delivery systems represent one of the best strategies to perform target drug transportation and decrease side effects in patients. As the thinnest materials, 2D materials have the highest specific surface areas among all known materials, and can act as large reservoirs and anchoring sites to efficiently load and deliver therapeutic agents[129,213] . Moreover, it is possible to take advantage of the outstanding physicochemical, optical, and electronic properties of the 2D materials to combine the drug delivery systems with cellular imaging, chemotherapy, photothermal (PPT) and photodynamic (PDT) therapies to develope smart drug delivery systems[214]. In these applications, the surface properties of the 2D materials play an important role in efficient drug loading. The GMs - graphene, GO and rGO - were the first 2D materials explored as carriers in drug delivery systems [215, 216, 217] by harnessing the surface properties. The surface of graphene is abundant in delocalized surface π electrons that can be used for effective drug loading of poorly soluble drugs (the most common drugs used in cancer therapies) *via* hydrophobic interactions and π–π stacking[216,218]. Additionally, the large surface area of graphene allows the high density functionalization of its surface via both covalent and non-covalent approach, improving the drugs loading[219]. However, GO is more widely used than graphene for drug delivery applications due to the presence of carboxylic, epoxy and hydroxide groups, which allow for wide range of reactions and functionalization opportunities. Furthermore, the surface of GO displays a coexistence of hydrophobic and hydrophilic properties, due to the sp^2 and sp^3 hybridized carbon domains in its structure, which enables this material to possess good water dispersity and biocompatibility, but also a high affinity for some drug molecules that are immiscible in aqueous media. However, in contrast with GO, graphene has more sp^2 hybridized carbon domains exhibiting a higher absorbance in the near-infrared region (NIR), which is favorable for the PPT and PDT applications[220].

A particular interest of drug delivery systems is to perform the release a sequence of drugs with defined kinetics and molar ratios to enhance the therapeutic effects while minimizing the dose to patients[221]. Recently, Schneible et al. achieved this concept by developing a nanocomposite based on GO nanosheets embedded in a Max8 peptide hydrogel, which provides controlled kinetics and molar ratios of release of doxorubicin (DOX) and gemcitabine (GEM)[221]. With this nanocomposite, the authors demonstrated the high DOX loading on GO and sustained release by pH (18.9% over 72 h and 31.4%

over 4 weeks) and a Max8 hydrogel with a capability to release GEM with faster kinetics and with 10-fold molar ratio to DOX. The nanocomposite based on DOX/GO@GEM/Max8 hydrogel matrix was tested against a triple negative breast cancer cell line, MDA-MB-231, and achieved a combination index of 0.093 ± 0.001; indicating a much stronger synergistic effect compared to the DOX–GEM combination as free drugs co-administered in solution (CI = 0.396 ± 0.034). This combination index value obtained by the DOX/GO@GEM/Max8 hydrogel nanocomposite was the lowest reported in the literature for this and similar drugs.

As a member of the TMDs family, MoS_2 shows very interesting application in drug delivery systems combined with PPT and PDT. This is due to the fact that a monolayer of MoS_2 has 7.8 times higher NIR absorbance than GO. In addition, the surface chemistry of MoS_2 is rich for functionalization, since MoS_2 has unsaturated d-orbitals, chemically active edge defects and sulfur vacancies, that acting as sites for introducing functional groups and ligands[222]. However MoS_2 demonstrated low serum stability and inefficient intracellular delivery[223,224]. A nice strategy to mitigate these issues and improve the biocompatibility and decreased even more the cytotoxicity is to perform the functionalization of the surface of Mos_2 with biocompatible materials and/or biomolecules. This was clearly demonstrated recently by Xie. M. *et al.*[225] . The authors showed the modification of the MoS_2 surface with egg yolk phospholipids (MoS_2-Lipid) to enhance the stability of the MoS_2 nanosheets under physiological conditions and to act as nanocarrier system for the treatment of tumors via the combination of chemotherapy and photothermal therapy. The MoS_2-Lipid demonstrated a loading rate of DOX of 104.4 %, and a release mediate by pH and NIR light. The non- covalent functionalization of the MoS_2 surface with lipids by coating, represents an easy strategy to improve the stability of MoS_2 nanosheets, but also enhanced the biocompatibility and the accumulation of the nanocarrier in mice tumors in vivo.

Another 2D material that has been drawing attention as an ideal candidate for drug delivery is h-BN, which possess many beneficial properties including surface chemical inertness, hierarchical surface porosity, high specific surface area, the low toxicity, and high thermal conductivity[129]. Fu, Z. et al[226], took advantage of the unique properties of h-BN to develop a multifunctional nanoplatform, co-carrying DOX and the heat shock protein inhibitor 17AAG, which can kill cancer cells and inhibit tumor growth at relatively low temperatures. The high surface area of h-BN allowed the high density functionalization with the cRGD peptide to target the αvβ3 integrin, which is over-expressed in the cells of tumors. The h-BN nanoplatform exhibited a high loading capacity for DOX (603 mg g^{-1}) with a drug release by pH and NIR controlled. The presence of 17AAG and the high thermal conductivity of the h-BN nanosheets, allowed for low temperature PTT to be combined with chemotherapy with DOX, resulting in highly effective anti-cancer activity of the multifunctional platform based on h-BN nanosheets.

Based on the combination of drug delivery and PPT- PDT process, many others 2D materials have been exploited in this purpose, mainly that have strong light absorption in NIR regions, such as MXens[227] and BP[172,228] as can be seen in the table 2.

3.3 – Biocompatibility and Biodegradability

The biocompatibility and biodegradability of the 2D materials are essential for their integration and use in biomedical applications, such as implantable devices, tissue engineering, drug delivery systems, among others. The biocompatibility of 2D materials is not only dependent on the surface properties of these materials, such as functionalization degree and reactive surface, but also the concentration, purity, size, shape, thickness and form of the 2D materials.[229,230,231] For example, a study performed by Mateti et al.[232] showed that micrometer-sized h-BN nanosheets possess *in vitro* biocompatibility against Osteoblast-like cells; however, nanosheets with a lateral size less than 1μm and a thickness below 100 nm were less biocompatible. It was suggested that this observation may be due to the unsaturated B atoms located at the nanosheet edges or on the surface of the material (in the case of defects) are present in a radical state, and triggering faster reactivity kinetics with other active atoms, such as oxygen, to generate ROS and leading to cell death. In this case, the larger lateral sized nanosheets of h-BN possess more exposed edges with unsaturated B atoms, and, thus, would decrease the biocompatibility of this 2D material.

In case of the GMs, graphene and its derivatives obtained by different methods, such as mechanical exfoliation, CVD or solution process (liquid and chemical exfoliation), can all exhibit different biocompatibility properties. Nanoflakes of chemically exfoliated graphene, micrometer size flakes of GO, or substrate bound CVD graphene will have dramatically different interactions and effects (if any) on live cells and tissue that can result in contradicting conclusions.[233] For example, a study performed by Park et al.[234] showed that graphene obtained by CVD on copper foil was an ideal substrate to promote the cardiomyogenic differentiation process of mesenchymal stem cells. Moreover, it was also found that the grown graphene did not exhibit any sign of cytotoxicity for the stem cell cultures; indicating that this method for obtaining graphene could be an approach towards the development of implantable biosensors based on CVD graphene.

The functionalization of the surface of 2D materials is a great strategy to improve the biocompatibility of these materials.[235,230] In this sense, GO poses as an ideal candidate due to their intrinsic oxygen functional groups at its surface. Jasim et al.[236] demonstrated that the intravenous injection of large amounts of GO nanosheets into mice resulted in an extensive urinary excretion, indicating a rapid transit across the glomerular filtration barrier (GFB), without causing any kidney (or other tissue)

damage. Similarly, it has been reported that the functionalization of the MoS_2 surface with lipoic acid and poly(ethylene glycol) (PEG) improved significantly its biocompatibility and physiological stability[237].
The investigation of the mechanisms and material parameters that are responsible for the biocompatibility of 2D materials, and the potential for the materials to induce any type of damage in the tissues, still warrants thorough investigation. This is the only way to ensure the safe use of 2D materials in biomedical applications. In this context, we can highlight government initiatives such as the GRAPHENE Flagship project[238], funded by the European Union, that has a work package (Health and Environment) related to study the safety and potential risks to the health of animals, humans and the environment, of the graphene and other 2D materials. These initiatives help to improve and seek new knowledge regarding the nanosafety of 2D materials, contributing to the future commercial implementation of these materials in the biomedical applications.

The biodegradability of 2D materials is other important parameter that needs to be very well investigated before its integration in biomedical applications. In particular, the biodegradaility has to be considered for some biomedical applications which may require long-term integration within the biological milieu[233], such as orthopedic or neuronal implants, catheters, wound healing agents, implantable biosensors and corneal devices. Moreover, for biomedical application such as drug delivery systems, the ability of 2D materials to biodegrade is very important and can be influenced by many factors, inlcuding the type of material, the degree of chemical functionalization, the aqueous dispersity and the redox potentials of the different oxidative environments. Thus, it is of utmost importance to consider all of these parameters when examining the biodegradability of 2D materials, and to find stratergies to enable, or promote, this aspect for commercial biotechnologies.[235] Recently, Bianco et al.[235] performed an elegant roadmap study examining the main parameters into the biodegradation of 2D materials. The surface defects, functional groups and chemical functionalization all played an important role in the promotion of the biodegradability. Furthermore, the authors introduced the concept of "degradation-by-design" which represents a great approach to improve the biodegradability of the 2D materials by the covalent modification of the material surface with appropriate molecules.

4. Future outlook and conclusions

From the early stages of discovery, to recent advancements in synthesis and surface engineering, there is no denying that tremendous progress and achievements have been made in the field of 2D materials. With such a diverse range of properties, and endless possibilities to 'mix and match', 2D materials have benefited many areas of research and technology. In particular, 2D materials have great potential for bio-applications that can have great impacts on healthcare and society.

Owing to its outstanding properties that arise from its dimensionality and surface interactions, 2D materials have levitated many intrinsic limitations of biomolecular and chemical sensing, such as low signals, slow bio-reaction times or events, and instability, and have enabled the realization of many platforms and devices with high sensitivity and selectivity. Surface engineering and functionalization techniques to modify and tune the electronic and optical properties have become a common approach to expand the family of 2D materials and to compensate for various drawbacks. Moreover, due to the success of 2D materials, there are continuous efforts in finding newer and novel 2D materials with potentially superior properties or more facile synthetic routes.

With this in mind, there are still several challenges and limitations that need to be addressed. Whilst 2D materials has been a trending topic for the past two decades, the commercial availability of healthcare devices and technologies based on 2D materials is currently still lacking. The key reason that hinders its market presence stems from large-scale production and standardization issues. As the properties of 2D materials are defined by its physical and atomic structures, it is essential that mass production of the materials have high uniformity (control on the number of layers, lateral size and defects of the nanosheets) such that there is no, or low, device-to-device variability. This is also particularly true for applications that require surface functionalization, where the amount/concentration of bioreceptors should be consistent in each sensor or device.

In addition, to have a competitive and economical edge, the synthesis methods should be low cost, yet with a high degree of controllability. The issue of low cost mass production is also another factor that hinders the commercial availability of 2D material-based biotechnologies. For platforms and devices that require pristine and uniform surfaces, like FETs, growth methods, such as chemical vapor deposition (CVD), are costly approaches to obtain high quality, yet low-yielding, 2D materials. To meet several growth parameters, such as high temperatures and pressures, expensive and specific instruments and facilities are typically required alongside the costs associated with hiring and training specialized personnel. On the other hand, solution based methods, such as ultrasonication assisted exfoliation, may be a cost effective and high-yielding approach. However, this represents only a reality for graphene and its derivatives; where some companies on the market are able to control the homogeneity of graphene and its derivatives from bath to batch. The mass production of 2D nanomaterials beyond graphene, such as the TMDs and h-BN, still pose as a challenge. Besides that, the implementation of the 2D materials in biomedical applications, such as tissue engineering and drug delivery system, require a strict quality control of the 2D nanosheets obtained by solution based methods. The use of the rigorous protocols that aim to purify and remove the remaining impurities from liquid chemical exfoliation process, such as acids, basis, and metallic ions, among others, from the resulting 2D dispersion needs to be performed. The

presence of chemical impurities, as well as the type of solvent and the pH value of the dispersion, can greatly affect the performance the 2D materials in the biomedical applications and even more affect its cytotoxicity. Whilst these drawbacks may be overlooked in research settings, translation of these processes to commercial products and mass production must be addressed.

Another issue, mainly related to *in vivo* and biomedical uses, is the stability and compatibility in biological environments for extended periods of time. Factors such as device or material degradation, due to exposure to complex biological media, toxicity, and prolonged use and its effects should be systematically evaluated prior to their use in everyday life.

In conclusion, while there are still several challenges and limitations to be faced, it is evident that the field of 2D materials has made tremendous progress and has had great impacts for biosensors and biomedical devices. In this review we highlight the importance of the surface and dimensionality of 2D materials and how it has influenced the design and development of many biotechnologies. We showed that the understanding of the surface properties (high surface area, surface roughness, chemical functionalities of the surface, surface charge, confinement of charge carriers, biocompatibility and among others), the dimensionality and shape of the 2D materials nanosheets is the key point to better explore the potential of these materials in the successful development of biotechnologies such as in biosensors, implants, tissue engineering, membranes and surfaces with antimicrobial and antifouling properties, among others. Thanks to the unique surface properties of the 2D materials it has been possible to develop biosensors with outstanding characteristics, never achieved before using materials at the bulk scale. Biosensors with impressive low limits of detection (fM, aM and even zM), miniaturized, integrated into the user`s skin, stable and with different functionalities have been developed taking advantage of the 2D materials surface properties. It is thanks to the constant strive of many researchers, both inside and outside of academia, to better understand the properties and mechanisms of 2D materials that enables the creation of novel strategies and engineering methods to push for the realization of advanced and future biotechnologies.

Acknowledgements:

We acknowledge financial support from EU Graphene Flagship Core 3 Project (No. 881603), from the Spanish MINECO under project MAT2017-87202-P. ICN2 is supported by the Severo Ochoa program from Spanish MINECO (Grant no. SEV-2013-0295) and by the CERCA Programme/Generalitat de Catalunya. E. P. N. acknowledges funding through the EU's Horizon 2020 research and innovation programme under the Marie Skłodowska-Curie grant agreement No. 754510. C. C. C. S acknowledges

funding through CAPES – PRINT (Programa Institucional de Internacionalização; Grant # 88887.310281/2018-00 and 88887.467442/2019-00).

Conflicts of Interests

There are no conflicts of interest to declare.

Author Profiles

Dr. Emily P. Nguyen received her PhD in 2017 from the Royal Melbourne Institute of Technology (RMIT) University, Australia. During that time, she also had a research stay at the University of California, Los Angeles (UCLA). Since 2018, she has held a post-doctoral position in the Nanobioelectronics and Biosensors Group at the Catalan Institute of Nanoscience and Nanotechnology (ICN2), Spain.. Her research interests include chemistry and functionalization of 2D materials for optoelectronic and electrochemical biosensors, and printed bioelectronics.

Dr. Cecília de Carvalho Castro Silva obtained her PhD at the University of Campinas (Unicamp), Campinas, Brazil (2015). Since January 2016, she has been assistant professor at MackGraphe - Graphene and Nanomaterials Research Center, Mackenzie Presbyterian University, São Paulo, Brazil. Currently, she is a visiting professor in the Nanobioelectronics and Biosensors Group at the Catalan Institute of Nanoscience and Nanotechnology (ICN2), Barcelona, Spain. She was included by Forbes-Brazil in the list "30 Under 30", of the 30 most talented youngsters under 30 years in 2016. Her research interests are dedicated to two-dimensional materials, biosensors and bioelectronics for health-care applications

Prof. Arben Merkoçi is an ICREA Research Professor and leader of the Nanobioelectronics and Biosensors Group in the Catalan Institute of Nanoscience and Nanotechnology (ICN2), Barcelona, Spain. Prof. Merkoçi is the co-founder of two spin-off companies: *GraphenicaLab*, devoted to graphene patterning, and *PaperDrop*, to clinical diagnostics. His research is focused on the integration of biological molecules and other species with micro- and nanostructures of interest in the design of novel (bio)sensors. He is also Co-Editor in Chief of *Biosensors and Bioelectronics*, and a member of the editorial board of *Electroanalysis*, *Microchimica Acta* and other journals.

References

1 K. S. Novoselov, *Science (80-.).*, 2004, **306**, 666–669.
2 C. W. Lee, J. M. Suh and H. W. Jang, *Front. Chem.*, 2019, **7**, 708.
3 A. Bolotsky, D. Butler, C. Dong, K. Gerace, N. R. Glavin, C. Muratore, J. A. Robinson and A. Ebrahimi, *ACS Nano*, 2019, **13**, 9781–9810.
4 S. Balendhran, S. Walia, M. Alsaif, E. P. Nguyen, J. Z. Ou, S. Zhuiykov, S. Sriram, M. Bhaskaran and K. Kalantar-Zadeh, *ACS Nano*, 2013, **7**, 9753–9760.
5 R. Kurapati, K. Kostarelos, M. Prato and A. Bianco, *Adv. Mater.*, 2016, 28, 6052–6074.
6 M. Chhowalla, H. S. Shin, G. Eda, L. J. Li, K. P. Loh and H. Zhang, *Nat. Chem.*, 2013, 5, 263–275.
7 J. H. Kim and M. Benelmekki, in *Frontiers of Nanoscience*, 2019, vol. 14, pp. 103–120.
8 N. Ashraf, M. Isa khan, A. Majid, M. Rafique and M. B. Tahir, *Chinese J. Phys.*, 2020, **66**, 246–257.
9 S. Z. Butler, S. M. Hollen, L. Cao, Y. Cui, J. A. Gupta, H. R. Gutiérrez, T. F. Heinz, S. S. Hong, J. Huang, A. F. Ismach, E. Johnston-Halperin, M. Kuno, V. V. Plashnitsa, R. D. Robinson, R. S. Ruoff, S. Salahuddin, J. Shan, L. Shi, M. G. Spencer, M. Terrones, W. Windl and J. E. Goldberger, *ACS Nano*, 2013, 7, 2898–2926.
10 X. Gan, H. Zhao, R. Schirhagl and X. Quan, *Microchim. Acta*, , DOI:10.1007/s00604-018-3005-1.
11 R. Boroujerdi, A. Abdelkader and R. Paul, *Nano-Micro Lett.*, 2020, **12**, 33.
12 Y. H. Wang, L. L. He, K. J. Huang, Y. X. Chen, S. Y. Wang, Z. H. Liu and D. Li, *Analyst*, 2019, **144**, 2849–2866.
13 Y. M. Lei, M. M. Xiao, Y. T. Li, L. Xu, H. Zhang, Z. Y. Zhang and G. J. Zhang, *Biosens. Bioelectron.*, 2017, **91**, 1–7.
14 N. Parvin, Q. Jin, Y. Wei, R. Yu, B. Zheng, L. Huang, Y. Zhang, L. Wang, H. Zhang, M. Gao, H. Zhao, W. Hu, Y. Li and D. Wang, *Adv. Mater.*, , DOI:10.1002/adma.201606755.
15 H. H. Xu, H. H. Deng, X. Q. Lin, Y. Y. Wu, X. L. Lin, H. P. Peng, A. L. Liu, X. H. Xia and W. Chen, *Microchim. Acta*, 2017, **184**, 3945–3951.
16 Q. Zhou, Y. Lin, J. Shu, K. Zhang, Z. Yu and D. Tang, *Biosens. Bioelectron.*, 2017, **98**, 15–21.
17 N. Chauhan, S. Chawla, C. S. Pundir and U. Jain, *Biosens. Bioelectron.*, , DOI:10.1016/j.bios.2016.06.047.
18 M. Ma, T. Zhe, Y. Ma, Z. Wang, Q. Chen and J. Wang, *Talanta*, 2018, **180**, 133–143.
19 X. Li, Y. Li, Q. Qiu, Q. Wen, Q. Zhang, W. Yang, L. Yuwen, L. Weng and L. Wang, *J. Colloid Interface Sci.*, , DOI:10.1016/j.jcis.2019.02.011.
20 N. F. Chiu and T. L. Lin, *Talanta*, 2018, **185**, 174–181.
21 D. Jiang, X. Du, L. Zhou, H. Li and K. Wang, *Anal. Chem.*, 2017, **89**, 4525–4531.
22 S. Mao, J. Chang, H. Pu, G. Lu, Q. He, H. Zhang and J. Chen, *Chem. Soc. Rev.*, 2017, **46**, 6872–6904.
23 W. Nie, Q. Wang, X. Yang, H. Zhang, Z. Li, L. Gao, Y. Zheng, X. Liu and K. Wang, *Anal. Chim. Acta*, 2017, **993**, 55–62.
24 H. Park, G. Han, S. W. Lee, H. Lee, S. H. Jeong, M. Naqi, A. AlMutairi, Y. J. Kim, J. Lee, W. Kim, S. Kim, Y. Yoon and G. Yoo, *ACS Appl. Mater. Interfaces*, 2017, **9**, 43490–43497.
25 S. Su, W. Cao, W. Liu, Z. Lu, D. Zhu, J. Chao, L. Weng, L. Wang, C. Fan and L. Wang, *Biosens. Bioelectron.*, 2017, **94**, 552–559.
26 D. Zhu, W. Liu, D. Zhao, Q. Hao, J. Li, J. Huang, J. Shi, J. Chao, S. Su and L. Wang, *ACS Appl. Mater. Interfaces*, 2017, **9**, 35597–35603.
27 Y. Guo, Y. Shu, A. Li, B. Li, J. Pi, J. Cai, H. Cai and Q. Gao, *J. Mater. Chem. B*, 2017, **5**, 5532–5538.
28 M. Shorie, V. Kumar, H. Kaur, K. Singh, V. K. Tomer and P. Sabherwal, *Microchim. Acta*, , DOI:10.1007/s00604-018-2705-x.
29 Y. Ju, X. Hu, Y. Zang, R. Cao and H. Xue, *Anal. Methods*, 2019, **11**, 2163–2169.
30 Y. Tan, M. Li, X. Ye, Z. Wang, Y. Wang and C. Li, *Sensors Actuators B Chem.*, 2018, **262**, 982–

990.
31 Y. Niu, R. Zou, H. A. Yones, X. Li, X. Li, X. Niu, Y. Chen, P. Li and W. Sun, *J. Chinese Chem. Soc.*, 2018, **65**, 1127–1135.
32 G. Hong, R. Chen, L. Xu, X. Lu, Z. Yang, G. Zhou, L. Li, W. Chen and H. Peng, *Anal. Chim. Acta*, 2020, **1099**, 52–59.
33 X. Li, X. Niu, W. Zhao, W. Chen, C. Yin, Y. Men, G. Li and W. Sun, *Electrochem. commun.*, 2018, **86**, 68–71.
34 Y. Chen, R. Ren, H. Pu, J. Chang, S. Mao and J. Chen, *Biosens. Bioelectron.*, 2017, **89**, 505–510.
35 J. Liu, L. Meng, Z. Fei, P. J. Dyson, X. Jing and X. Liu, *Biosens. Bioelectron.*, 2017, **90**, 69–74.
36 J. Ji, J. Wen, Y. Shen, Y. Lv, Y. Chen, S. Liu, H. Ma and Y. Zhang, *J. Am. Chem. Soc.*, 2017, **139**, 11698–11701.
37 S. Kumar, Y. Lei, N. H. Alshareef, M. A. Quevedo-Lopez and K. N. Salama, *Biosens. Bioelectron.*, 2018, **121**, 243–249.
38 P.-P. Li, X.-P. Liu, C.-J. Mao, B.-K. Jin and J.-J. Zhu, *Anal. Chim. Acta*, 2019, **1048**, 42–49.
39 J.-M. Jeong, M. Yang, D. S. Kim, T. J. Lee, B. G. Choi and D. H. Kim, *J. Colloid Interface Sci.*, 2017, **506**, 379–385.
40 T. Yang, M. Chen, Q. Kong, X. Luo and K. Jiao, *Biosens. Bioelectron.*, 2017, **89**, 538–544.
41 R. Kumari, F. Opoku, A. O. Osikoya, W. W. Anku, S. K. Shukla and P. P. Govender, *Mater. Chem. Phys.*, 2019, **226**, 129–140.
42 S. Augustine, P. Kumar and B. D. Malhotra, *ACS Appl. Bio Mater.*, 2019, **2**, 5366–5378.
43 I. Alam, L. M. Guiney, M. C. Hersam and I. Chowdhury, *Environ. Sci. Nano*, 2018, **5**, 1628–1639.
44 T. I. Kim, J. Kim, I.-J. Park, K.-O. Cho and S.-Y. Choi, *2D Mater.*, 2019, **6**, 025025.
45 P. Cheng, Y. Chen, X. Yan, Y. Wang and W. Z. Lang, *ChemSusChem*, 2019, **12**, 275–282.
46 Z. Xiong, X. Zhang, S. Zhang, L. Lei, W. Ma, D. Li, W. Wang, Q. Zhao and B. Xing, *Ecotoxicol. Environ. Saf.*, 2018, **161**, 507–514.
47 Z. Sun, Y. Zhang, H. Yu, C. Yan, Y. Liu, S. Hong, H. Tao, A. W. Robertson, Z. Wang and A. A. H. Pádua, *Nanoscale*, 2018, **10**, 12543–12553.
48 N. Yadav, A. Dubey, S. Shukla, C. P. Saini, G. Gupta, R. Priyadarshini and B. Lochab, *ACS Omega*, 2017, **2**, 3070–3082.
49 M. P. Romero, V. S. Marangoni, C. G. de Faria, I. S. Leite, C. de C. C. e. Silva, C. M. Maroneze, M. A. Pereira-da-Silva, V. S. Bagnato and N. M. Inada, *Front. Microbiol.*, , DOI:10.3389/fmicb.2019.02995.
50 D. Prema, J. Prakash, S. Vignesh, P. Veluchamy, C. Ramachandran, D. B. Samal, D. H. Oh, S. Sahabudeen and G. Devanand Venkatasubbu, *Appl. Nanosci.*, 2019, **10**, 827–849.
51 M. Muthuchamy, R. Govindan, K. Shine, V. Thangasamy, N. S. Alharbi, M. Thillaichidambaram, J. M. Khaled, J.-L. Wen and K. F. Alanzi, *Carbohydr. Polym.*, 2020, **230**, 115646.
52 G. Choe, S. Oh, J. M. Seok, S. A. Park and J. Y. Lee, *Nanoscale*, 2019, **11**, 23275–23285.
53 L. Wang, M. Fang, Y. Xia, J. Hou, X. Nan, B. Zhao and X. Wang, *RSC Adv.*, 2020, **10**, 10118–10128.
54 X. Liu, A. L. Miller, S. Park, M. N. George, B. E. Waletzki, H. Xu, A. Terzic and L. Lu, *ACS Appl. Mater. Interfaces*, 2019, **11**, 23558–23572.
55 K. Chen, Y. Chen, Q. Deng, S. H. Jeong, T. S. Jang, S. Du, H. E. Kim, Q. Huang and C. M. Han, *Mater. Lett.*, 2018, **229**, 114–117.
56 S. Nagarajan, H. Belaid, C. Pochat-Bohatier, C. Teyssier, I. Iatsunskyi, E. Coy, S. Balme, D. Cornu, P. Miele, N. S. Kalkura, V. Cavaillès and M. Bechelany, *ACS Appl. Mater. Interfaces*, 2017, **9**, 33695–33706.
57 B. Farshid, G. Lalwani, M. Shir Mohammadi, J. Simonsen and B. Sitharaman, *J. Biomed. Mater. Res. Part B Appl. Biomater.*, 2017, **105**, 406–419.
58 L. He, S. Sarkar, A. Barras, R. Boukherroub, S. Szunerits and D. Mandler, *Chem. Commun.*, 2017, **53**, 4022–4025.
59 T. Yin, J. Liu, Z. Zhao, Y. Zhao, L. Dong, M. Yang, J. Zhou and M. Huo, *Adv. Funct. Mater.*,

2017, **27**, 1–12.
60 S. Han, F. Teng, Y. Wang, L. Su, Q. Leng and H. Jiang, *RSC Adv.*, 2020, **10**, 10980–10988.
61 C. C. Cheng, A. A. Muhabie, S. Y. Huang, C. Y. Wu, B. T. Gebeyehu, A. W. Lee, J. Y. Lai and D. J. Lee, *Nanoscale*, 2019, **11**, 10393–10401.
62 Y. Yang, J. Wu, D. H. Bremner, S. Niu, Y. Li, X. Zhang, X. Xie and L. M. Zhu, *Colloids Surfaces B Biointerfaces*, , DOI:10.1016/j.colsurfb.2019.110585.
63 G. Liu, J. Zou, Q. Tang, X. Yang, Y. Zhang, Q. Zhang, W. Huang, P. Chen, J. Shao and X. Dong, *ACS Appl. Mater. Interfaces*, 2017, **9**, 40077–40086.
64 L. Jin, P. Hu, Y. Wang, L. Wu, K. Qin, H. Cheng, S. Wang, B. Pan, H. Xin, W. Zhang and X. Wang, *Adv. Mater.*, 2020, **32**, 1906050.
65 X. Ding, C. Hong, G. Zhang, J. Liu, H. Ouyang, M. Wang, L. Dong, W. Zhang, H. Xin and X. Wang, *Nanoscale Horizons*, 2019, **4**, 1277–1285.
66 J. Wang, G. Li and L. Li, in *Two-dimensional Materials - Synthesis, Characterization and Potential Applications*, InTech, 2016.
67 A. Zavabeti, A. Jannat, L. Zhong, A. A. Haidry, Z. Yao and J. Z. Ou, *Nano-Micro Lett.*, 2020, **12**, 66.
68 J. Sophia Ponraj, Z.-Q. Xu, S. Chander Dhanabalan, al -, F. Wang, Z. Wang and Q. Wang, *2D Mater.*, 2016, **3**, 042001.
69 R. Podila, A. Rao, P. Puneet, S. Bhattacharya, S. S. K. Mallineni, A. Srivastava, F. Liu, J. Taha-Tijerina, L. Peña-Parás, D. Maldonado-Cortes, G. Qin, M. Hu, Y. Alaskar, S. Arafin, K. Wang, Q. Chi, M. Xue, F. Li, R. Cheung and L. Guangshe, *Two-dimensional Materials- Synthesis, Characterization and Potential Applications*, INTECH, 2016.
70 Q. H. Wang, K. Kalantar-Zadeh, A. Kis, J. N. Coleman and M. S. Strano, *Nat. Nanotechnol.*, 2012, 7, 699–712.
71 H. Zhang, *ACS Nano*, 2015, **9**, 9451–9469.
72 C. Anichini, W. Czepa, D. Pakulski, A. Aliprandi, A. Ciesielski and P. Samorì, *Chem. Soc. Rev.*, 2018, 47, 4860–4908.
73 P. Bazylewski, S. Van Middelkoop, R. Divigalpitiya and G. Fanchini, *ACS Omega*, 2020, **5**, 643–649.
74 D. Akinwande, C. J. Brennan, J. S. Bunch, P. Egberts, J. R. Felts, H. Gao, R. Huang, J. S. Kim, T. Li, Y. Li, K. M. Liechti, N. Lu, H. S. Park, E. J. Reed, P. Wang, B. I. Yakobson, T. Zhang, Y. W. Zhang, Y. Zhou and Y. Zhu, *Extrem. Mech. Lett.*, 2017, 13, 42–77.
75 R. Zhang and R. Cheung, in *Two-dimensional Materials - Synthesis, Characterization and Potential Applications*, InTech, 2016.
76 C. Lee, X. Wei, J. W. Kysar and J. Hone, *Science (80-.).*, 2008, **321**, 385–388.
77 S. P. Koenig, N. G. Boddeti, M. L. Dunn and J. S. Bunch, *Nat. Nanotechnol.*, 2011, **6**, 543–546.
78 X. Cao, A. Halder, Y. Tang, C. Hou, H. Wang, J. O. Duus and Q. Chi, *Mater. Chem. Front.*, 2018, 2, 1944–1986.
79 H. Kim and J. H. Ahn, *Carbon N. Y.*, 2017, **120**, 244–257.
80 S. Begum, A. Pramanik, D. Davis, S. Patibandla, K. Gates, Y. Gao and P. C. Ray, *ACS Omega*, 2020, **5**, 3116–3130.
81 M. Y. Li, C. H. Chen, Y. Shi and L. J. Li, *Mater. Today*, 2016, **19**, 322–335.
82 Y. Gong, S. Lei, G. Ye, B. Li, Y. He, K. Keyshar, X. Zhang, Q. Wang, J. Lou, Z. Liu, R. Vajtai, W. Zhou and P. M. Ajayan, *Nano Lett.*, 2015, **15**, 6135–6141.
83 I. V. Sankar, J. Jeon, S. K. Jang, J. H. Cho, E. Hwang and S. Lee, *Nano*, 2019, 14.
84 A. K. Geim and I. V. Grigorieva, *Nature*, 2013, 499, 419–425.
85 M. Velicky and P. Toth, *Appl. Mater. Today*, 2017, **8**, 68–103.
86 P. P. Li, X. P. Liu, C. J. Mao, B. K. Jin and J. J. Zhu, *Anal. Chim. Acta*, 2019, **1048**, 42–49.
87 R. Vargas-Bernal, *Sensors (Basel).*, 2019, **19**, 1295.
88 M. G. Stanford, P. D. Rack and D. Jariwala, *npj 2D Mater. Appl.*, 2018, **2**, 20.
89 V. K. Sangwan and M. C. Hersam, *Annu. Rev. Phys. Chem.*, 2018, **69**, 299–325.

90 H. Huang, R. Jiang, Y. Feng, H. Ouyang, N. Zhou, X. Zhang and Y. Wei, *Nanoscale*, 2020, 12, 1325–1338.
91 L. Syedmoradi, A. Ahmadi, M. L. Norton and K. Omidfar, *Microchim. Acta*, , DOI:10.1007/s00604-019-3850-6.
92 Y. Chen, K. Yang, B. Jiang, J. Li, M. Zeng and L. Fu, *J. Mater. Chem. A*, 2017, 5, 8187–8208.
93 J. Li, Z. Wei and J. Kang, *Two-Dimensional Semicond.*, 2020, 35–53.
94 M. Xiong, Q. Rong, H. min Meng and X. bing Zhang, *Biosens. Bioelectron.*, 2017, **89**, 212–223.
95 L. Daukiya, J. Seibel and S. De Feyter, *Adv. Phys. X*, 2019, **4**, 1625723.
96 S. Trivedi, K. Lobo and H. S. S. Ramakrishna Matte, in *Woodhead Publishing Series in Electronic and Optical Materials*, eds. M. Hywel, C. S. Rout and D. J. B. T.-F. and S. A. of 2D M. Late, Woodhead Publishing, 2019, pp. 25–90.
97 P. V Shinde and M. K. Singh, in *Woodhead Publishing Series in Electronic and Optical Materials*, eds. M. Hywel, C. S. Rout and D. J. B. T.-F. and S. A. of 2D M. Late, Woodhead Publishing, 2019, pp. 91–143.
98 T. Niu, J. Zhang and W. Chen, *ChemNanoMat*, 2019, **5**, 6–23.
99 J. Hong, C. Jin, J. Yuan and Z. Zhang, *Adv. Mater.*, , DOI:10.1002/adma.201606434.
100 Y. Qu, F. He, C. Yu, X. Liang, D. Liang, L. Ma and Q. Zhang, *Mater. Sci. Eng. C*, 2018, **90**, 764–780.
101 S. Najmaei, J. Yuan, J. Zhang, P. Ajayan and J. Lou, *Acc. Chem. Res.*, 2015, **48**, 31–40.
102 M. Pumera, *Mater. Today*, 2011, **14**, 308–315.
103 Y. Chen, S. Huang, X. Ji, K. Adepalli, K. Yin, X. Ling, X. Wang, J. Xue, M. Dresselhaus, J. Kong and B. Yildiz, *ACS Nano*, 2018, **12**, 2569–2579.
104 L. Tao, X. Duan, C. Wang, X. Duan and S. Wang, *Chem. Commun.*, 2015, **51**, 7470–7473.
105 H. Li, C. Tsai, A. L. Koh, L. Cai, A. W. Contryman, A. H. Fragapane, J. Zhao, H. S. Han, H. C. Manoharan, F. Abild-Pedersen, J. K. Nørskov and X. Zheng, *Nat. Mater.*, 2016, **15**, 48–53.
106 S. Ramaraj, M. Sakthivel, S. M. Chen, B. S. Lou and K. C. Ho, *ACS Appl. Mater. Interfaces*, 2019, **11**, 7862–7871.
107 X. Zhao, X. Dai, C. Xia, T. Wang and Y. Peng, *Solid State Commun.*, 2015, **215**–**216**, 1–4.
108 G. Maduraiveeran, M. Sasidharan and V. Ganesan, *Biosens. Bioelectron.*, 2018, **103**, 113–129.
109 K. Kalantar-Zadeh and J. Z. Ou, *ACS Sensors*, 2016, 1, 5–16.
110 G. Guan and M. Han, *Adv. Sci.*, 2019, **6**, 1901837.
111 C. Zhu, D. Du and Y. Lin, *Biosens. Bioelectron.*, 2017, **89**, 43–55.
112 S. Varghese, S. Varghese, S. Swaminathan, K. Singh and V. Mittal, *Electronics*, 2015, **4**, 651–687.
113 F. Vulcano, A. Kovtun, C. Bettini, Z. Xia, A. Liscio, F. Terzi, A. Heras, A. Colina, B. Zanfrognini, M. Melucci, V. Palermo and C. Zanardi, *2D Mater.*, , DOI:10.1088/2053-1583/ab734f.
114 X. S. Chu, A. Yousaf, D. O. Li, A. A. Tang, A. Debnath, D. Ma, A. A. Green, E. J. G. Santos and Q. H. Wang, *Chem. Mater.*, 2018, **30**, 2112–2128.
115 P. G. Moses, J. J. Mortensen, B. I. Lundqvist and J. K. Nørskov, *J. Chem. Phys.*, 2009, **130**, 104709.
116 E. P. Nguyen, B. J. Carey, C. J. Harrison, P. Atkin, K. J. Berean, E. Della Gaspera, J. Z. Ou, R. B. Kaner, K. Kalantar-Zadeh and T. Daeneke, *Nanoscale*, , DOI:10.1039/c6nr04326g.
117 V. Georgakilas, M. Otyepka, A. B. Bourlinos, V. Chandra, N. Kim, K. C. Kemp, P. Hobza, R. Zboril and K. S. Kim, *Chem. Rev.*, 2012, **112**, 6156–6214.
118 S. Kumar, S. Kaushik, R. Pratap and S. Raghavan, *ACS Appl. Mater. Interfaces*, 2015, **7**, 2189–2194.
119 A. Cagliani, D. M. A. Mackenzie, L. K. Tschammer, F. Pizzocchero, K. Almdal and P. Bøggild, *Nano Res.*, 2014, **7**, 743–754.
120 A. Salehi-Khojin, D. Estrada, K. Y. Lin, M.-H. Bae, F. Xiong, E. Pop and R. I. Masel, *Adv. Mater.*, 2012, **24**, 53–57.
121 J. Ma, M. Zhang, L. Dong, Y. Sun, Y. Su, Z. Xue and Z. Di, *AIP Adv.*, 2019, **9**, 075207.
122 N. Bhalla, P. Jolly, N. Formisano and P. Estrela, *Essays Biochem.*, 2016, **60**, 1–8.

123 S. Cheng, S. Hideshima, S. Kuroiwa, T. Nakanishi and T. Osaka, *Sensors Actuators, B Chem.*, 2015, **212**, 329–334.
124 M. Huang, H. Li, H. He, X. Zhang and S. Wang, *Anal. Methods*, 2016, **8**, 7413–7419.
125 R. Seeber, L. Pigani, F. Terzi and C. Zanardi, *Electrochim. Acta*, 2015, 179, 350–363.
126 Y. Zang, J. Lei and H. Ju, *Biosens. Bioelectron.*, 2017, 96, 8–16.
127 H. Y. Lin, W. H. Chen and C. H. Huang, *Graphene in electrochemical biosensors*, Elsevier Inc., 2019.
128 K. Shavanova, Y. Bakakina, I. Burkova, I. Shtepliuk, R. Viter, A. Ubelis, V. Beni, N. Starodub, R. Yakimova and V. Khranovskyy, *Sensors*, 2016, **16**, 223.
129 T. Hu, X. Mei, Y. Wang, X. Weng, R. Liang and M. Wei, *Sci. Bull.*, 2019, **64**, 1707–1727.
130 A. V. Pradeep, S. V. Satya Prasad, L. V. Suryam and P. Prasanna Kumari, *Mater. Today Proc.*, 2019, **19**, 380–383.
131 B. Liu and K. Zhou, *Prog. Mater. Sci.*, 2019, 100, 99–169.
132 S. K. Vashist and J. H. T. Luong, *Carbon N. Y.*, 2015, 84, 519–550.
133 F. Wang, C. Yang, C. Duan, D. Xiao, Y. Tang and J. Zhu, *J. Electrochem. Soc.*, 2015, **162**, B16–B21.
134 H. U. Kim, H. Y. Kim, H. Seok, V. Kanade, H. Yoo, K. Y. Park, J. H. Lee, M. H. Lee and T. Kim, *Anal. Chem.*, 2020, **92**, 6327–6333.
135 T. Wang, H. Zhu, J. Zhuo, Z. Zhu, P. Papakonstantinou, G. Lubarsky, J. Lin and M. Li, *Anal. Chem.*, 2013, **85**, 10289–10295.
136 J. M. Jeong, M. H. Yang, D. S. Kim, T. J. Lee, B. G. Choi and D. H. Kim, *J. Colloid Interface Sci.*, 2017, **506**, 379–385.
137 T. Yang, M. Chen, Q. Kong, X. Luo and K. Jiao, *Biosens. Bioelectron.*, 2017, **89**, 538–544.
138 Y. N. Zheng, W. Bin Liang, C. Y. Xiong, Y. Zhuo, Y. Q. Chai and R. Yuan, *Anal. Chem.*, 2017, **89**, 9445–9451.
139 W. W. Zhao, J. J. Xu and H. Y. Chen, *Chem. Soc. Rev.*, 2015, 44, 729–741.
140 M. Wang, H. Yin, Y. Zhou, C. Sui, Y. Wang, X. Meng, G. I. N. Waterhouse and S. Ai, *Biosens. Bioelectron.*, 2019, **128**, 137–143.
141 Y.-C. Syu, W.-E. Hsu and C.-T. Lin, *ECS J. Solid State Sci. Technol.*, , DOI:10.1149/2.0291807jss.
142 C. S. Lee, S. Kyu Kim and M. Kim, *Sensors*, 2009, **9**, 71111–7131.
143 M. Dankerl, M. V. Hauf, A. Lippert, L. H. Hess, S. Birner, I. D. Sharp, A. Mahmood, P. Mallet, J. Y. Veuillen, M. Stutzmann and J. A. Garrido, *Adv. Funct. Mater.*, , DOI:10.1002/adfm.201000724.
144 L. H. Hess, M. Seifert and J. A. Garrido, *Proc. IEEE*, 2013, **101**, 1780–1792.
145 G. Seo, G. Lee, M. J. Kim, S. H. Baek, M. Choi, K. B. Ku, C. S. Lee, S. Jun, D. Park, H. G. Kim, S. J. Kim, J. O. Lee, B. T. Kim, E. C. Park and S. Il Kim, *ACS Nano*, 2020, **14**, 5135–5142.
146 E. Stern, R. Wagner, F. J. Sigworth, R. Breaker, T. M. Fahmy and M. A. Reed, *Nano Lett.*, 2007, **7**, 3405–3409.
147 G. S. Kulkarni and Z. Zhong, *Nano Lett.*, 2012, **12**, 719–723.
148 M. T. Hwang, M. Heiranian, Y. Kim, S. You, J. Leem, A. Taqieddin, V. Faramarzi, Y. Jing, I. Park, A. M. van der Zande, S. Nam, N. R. Aluru and R. Bashir, *Nat. Commun.*, , DOI:10.1038/s41467-020-15330-9.
149 B. Radisavljevic, A. Radenovic, J. Brivio, V. Giacometti and A. Kis, *Nat. Nanotechnol.*, 2011, **6**, 147–150.
150 M. Chhowalla, D. Jena and H. Zhang, *Nat. Rev. Mater.*, 2016, 16052.
151 H. O. H. Churchill and P. Jarillo-Herrero, *Nat. Nanotechnol.*, 2014, **9**, 330–331.
152 B. N. Shivananju, H. Y. Hoh, W. Yu and Q. Bao, *Optical biochemical sensors based on 2D materials*, Elsevier Ltd, 2019.
153 B. N. Shivananju, W. Yu, Y. Liu, Y. Zhang, B. Lin, S. Li and Q. Bao, *Adv. Funct. Mater.*, , DOI:10.1002/adfm.201603918.

154 C. Zhu, D. Du and Y. Lin, *2D Mater.*, 2015, **2**, 32004.
155 B. N. Shivananju, H. Y. Hoh, W. Yu and Q. Bao, in *Fundamentals and Sensing Applications of 2D Materials*, Elsevier, 2019, pp. 379–406.
156 Z. Salamon, H. A. MacLeod and G. Tollin, *Biochim. Biophys. Acta - Rev. Biomembr.*, 1997, 1331, 117–129.
157 G. Xia, C. Zhou, S. Jin, C. Huang, J. Xing and Z. Liu, *Sensors*, 2019, **19**, 1198.
158 T. Xue, W. Liang, Y. Li, Y. Sun, Y. Xiang, Y. Zhang, Z. Dai, Y. Duo, L. Wu, K. Qi, B. N. Shivananju, L. Zhang, X. Cui, H. Zhang and Q. Bao, *Nat. Commun.*, 2019, **10**, 1–9.
159 X. Chia, A. Y. S. Eng, A. Ambrosi, S. M. Tan and M. Pumera, *Chem. Rev.*, 2015, **115**, 11941–11966.
160 S. Su, C. Zhang, L. Yuwen, J. Chao, X. Zuo, X. Liu, C. Song, C. Fan and L. Wang, *ACS Appl. Mater. Interfaces*, 2014, **6**, 18735–18741.
161 J. Zhao, Z. Zhang, S. Yang, H. Zheng and Y. Li, *J. Alloys Compd.*, 2013, **559**, 87–91.
162 J. Kim, S. Byun, A. J. Smith, J. Yu and J. Huang, *J. Phys. Chem. Lett.*, 2013, **4**, 1227–1232.
163 M. Shorie, V. Kumar, H. Kaur, K. Singh, V. K. Tomer and P. Sabherwal, *Microchim. Acta*, 2018, **185**, 158.
164 N. I. Khan and E. Song, *Micromachines*, 2020, **11**, 220.
165 P. M. Neema, A. M. Tomy and J. Cyriac, *TrAC Trends Anal. Chem.*, 2020, **124**, 115797.
166 R.-M. Kong, L. Ding, Z. Wang, J. You and F. Qu, *Anal. Bioanal. Chem.*, 2015, **407**, 369–377.
167 H. Yang, X. Jie, L. Wang, Y. Zhang, M. Wang and W. Wei, *Microchim. Acta*, 2018, **185**, 512.
168 A. Zamora-Gálvez, E. Morales-Narváez, J. Romero and A. Merkoçi, *Biosens. Bioelectron.*, 2018, **100**, 208–213.
169 X. Li, J. Shan, W. Zhang, S. Su, L. Yuwen and L. Wang, *Small*, 2017, **13**, 1602660.
170 S. Liu, X. Pan and H. Liu, *Angew. Chemie Int. Ed.*, 2020, **59**, 5890–5900.
171 V. Yadav, S. Roy, P. Singh, Z. Khan and A. Jaiswal, *Small*, 2019, **15**, 1–33.
172 X. Qian, Z. Gu and Y. Chen, *Mater. Horizons*, 2017, **4**, 800–816.
173 S. Szunerits and R. Boukherroub, *J. Mater. Chem. B*, 2016, 4, 6892–6912.
174 X. Yang, J. Li, T. Liang, C. Ma, Y. Zhang, H. Chen, N. Hanagata, H. Su and M. Xu, *Nanoscale*, 2014, **6**, 10126–10133.
175 K. Huang, Z. Li, J. Lin, G. Han and P. Huang, *Chem. Soc. Rev.*, 2018, **47**, 5109–5124.
176 O. Akhavan and E. Ghaderi, *ACS Nano*, , DOI:10.1021/nn101390x.
177 X. Zou, L. Zhang, Z. Wang and Y. Luo, *J. Am. Chem. Soc.*, , DOI:10.1021/jacs.5b11411.
178 K. Hossain, M. Rafatullah, S. Z. Abbas, A. Ahmad, N. Ismail and A. Y. Maruthi, in *Micro and Nano Technologies*, eds. M. Jawaid, A. Ahmad and D. B. T.-G.-B. N. for E. and E. A. Lokhat, Elsevier, 2019, pp. 293–314.
179 Y. Tu, M. Lv, P. Xiu, T. Huynh, M. Zhang, M. Castelli, Z. Liu, Q. Huang, C. Fan, H. Fang and R. Zhou, *Nat. Nanotechnol.*, , DOI:10.1038/nnano.2013.125.
180 B. Luan, T. Huynh, L. Zhao and R. Zhou, *ACS Nano*, , DOI:10.1021/nn506011j.
181 O. Akhavan and E. Ghaderi, *Carbon N. Y.*, 2012, **50**, 1853–1860.
182 J. D. West and L. J. Marnett, *Chem. Res. Toxicol.*, 2006, **19**, 173–194.
183 M. D. Rojas-Andrade, G. Chata, D. Rouholiman, J. Liu, C. Saltikov and S. Chen, *Nanoscale*, 2017, 9, 994–1006.
184 A. Gusev, O. Zakharova, I. Vasyukova, D. S. Muratov, I. Rybkin, D. Bratashov, A. Lapanje, I. Il'inikh, E. Kolesnikov and D. Kuznetsov, *Mater. Sci. Eng. C*, 2019, **99**, 275–281.
185 S. Liu, T. H. Zeng, M. Hofmann, E. Burcombe, J. Wei, R. Jiang, J. Kong and Y. Chen, *ACS Nano*, 2011, **5**, 6971–6980.
186 I. E. Mejías Carpio, C. M. Santos, X. Wei and D. F. Rodrigues, *Nanoscale*, 2012, **4**, 4746–4756.
187 L. Mei, S. Zhu, W. Yin, C. Chen, G. Nie, Z. Gu and Y. Zhao, *Theranostics*, 2020, **10**, 757–781.
188 M. Emanet, Ö. Sen, I. Ç. Taşkin and M. Çulha, *Front. Bioeng. Biotechnol.*, 2019, 7.
189 K. Rasool, K. A. Mahmoud, D. J. Johnson, M. Helal, G. R. Berdiyorov and Y. Gogotsi, *Sci. Rep.*, 2017, **7**, 1–11.

190 R. Wu, X. Ou, R. Tian, J. Zhang, H. Jin, M. Dong, J. Li and L. Liu, *Nanoscale*, 2018, **10**, 20162–20170.
191 Q. Xu, P. Zhu, J. Zhang, Y. Liu, L. Cai, H. Jiang, M. Ji and J. Chen, *Mater. Lett.*, 2020, **271**, 127809.
192 T. I. Kim, J. Kim, I. J. Park, K. O. Cho and S. Y. Choi, *2D Mater.*, , DOI:10.1088/2053-1583/ab070e.
193 Z. Khatoon, C. D. McTiernan, E. J. Suuronen, T. F. Mah and E. I. Alarcon, *Heliyon*, 2018, **4**, e01067.
194 F. Ghilini, D. E. Pissinis, A. Miñán, P. L. Schilardi and C. Diaz, *ACS Biomater. Sci. Eng.*, 2019, **5**, 4920–4936.
195 M. Chhowalla and G. A. J. Amaratunga, *Nature*, , DOI:10.1038/35025020.
196 J. K. Yang, H. R. Lee, I. J. Hwang, H. I. Kim, D. Bin Yim and J. H. Kim, *Adv. Healthc. Mater.*, 2018, **7**, 2–7.
197 J. Jang, Y. Choi, M. Tanaka and J. Choi, *J. Ind. Eng. Chem.*, 2020, **83**, 46–52.
198 J. Zheng, J. Li, L. Zhang, X. Chen, Y. Yu and H. Huang, *J. Mater. Sci.*, 2020.
199 B. K. Gu, D. J. Choi, S. J. Park, Y. Kim and C. Kim, *Cutting-Edge Enabling Technologies for Regenerative Medicine*, 2018, vol. 1078.
200 J. Zhang, H. Chen, M. Zhao, G. Liu and J. Wu, *Nano Res.*, , DOI:10.1007/s12274-020-2835-4.
201 O. Erol, I. Uyan, M. Hatip, C. Yilmaz, A. B. Tekinay and M. O. Guler, *Nanomedicine Nanotechnology, Biol. Med.*, 2018, **14**, 2433–2454.
202 B. Lu, T. Li, H. Zhao, X. Li, C. Gao, S. Zhang and E. Xie, *Nanoscale*, , DOI:10.1039/c2nr11958g.
203 V. Agarwal and K. Chatterjee, *Nanoscale*, 2018, **10**, 16365–16397.
204 H. Zanin, E. Saito, F. R. Marciano, H. J. Ceragioli, A. E. C. Granato, M. Porcionatto and A. O. Lobo, *J. Mater. Chem. B*, , DOI:10.1039/c3tb20550a.
205 V. Rosa, H. Xie, N. Dubey, T. T. Madanagopal, S. S. Rajan, J. L. P. Morin, I. Islam and A. H. Castro Neto, *Dent. Mater.*, , DOI:10.1016/j.dental.2016.05.008.
206 J. J. Lee, Y. C. Shin, S. J. Song, J. M. Cha, S. W. Hong, Y. J. Lim, S. J. Jeong, D. W. Han and B. Kim, *Coatings*, , DOI:10.3390/coatings8010013.
207 J. Li, G. Wang, H. Geng, H. Zhu, M. Zhang, Z. Di, X. Liu, P. K. Chu and X. Wang, *ACS Appl. Mater. Interfaces*, , DOI:10.1021/acsami.5b06639.
208 Y. Li, X. Zhang, C. Dai, Y. Yin, L. Gong, W. Pan, R. Huang, Y. Bu, X. Liao, K. Guo and F. Gao, *ACS Biomater. Sci. Eng.*, 2020, **6**, 3015–3025.
209 J. R. Choi, K. W. Yong, J. Y. Choi, A. Nilghaz, Y. Lin, J. Xu and X. Lu, *Theranostics*, 2018, **8**, 1005–1026.
210 M. G. Raucci, I. Fasolino, M. Caporali, M. Serrano-Ruiz, A. Soriente, M. Peruzzini and L. Ambrosio, *ACS Appl. Mater. Interfaces*, , DOI:10.1021/acsami.8b21592.
211 X. Liu, A. L. Miller, S. Park, M. N. George, B. E. Waletzki, H. Xu, A. Terzic and L. Lu, *ACS Appl. Mater. Interfaces*, 2019, **11**, 23558–23572.
212 K. Huang, J. Wu and Z. Gu, *ACS Appl. Mater. Interfaces*, 2019, **11**, 2908–2916.
213 L. Fusco, A. Gazzi, G. Peng, Y. Shin, S. Vranic, D. Bedognetti, F. Vitale, A. Yilmazer, X. Feng, B. Fadeel, C. Casiraghi and L. G. Delogu, *Theranostics*, 2020, **10**, 5435–5488.
214 H. Zhang, T. Fan, W. Chen, Y. Li and B. Wang, *Bioact. Mater.*, 2020, **5**, 1071–1086.
215 X. Sun, Z. Liu, K. Welsher, J. T. Robinson, A. Goodwin, S. Zaric and H. Dai, *Nano Res.*, 2008, **1**, 203–212.
216 S. Goenka, V. Sant and S. Sant, *J. Control. Release*, 2014, **173**, 75–88.
217 J. Liu, L. Cui and D. Losic, *Acta Biomater.*, 2013, **9**, 9243–9257.
218 L. Cheng, X. Wang, F. Gong, T. Liu and Z. Liu, *Adv. Mater.*, 2020, **32**, 1902333.
219 B. L. Li, R. Li, H. L. Zou, K. Ariga, N. B. Li and D. T. Leong, *Mater. Horizons*, 2020, **7**, 455–469.
220 G. Reina, J. M. González-Domínguez, A. Criado, E. Vázquez, A. Bianco and M. Prato, *Chem. Soc. Rev.*, 2017, **46**, 4400–4416.
221 J. D. Schneible, K. Shi, A. T. Young, S. Ramesh, N. He, C. E. Dowdey, J. M. Dubnansky, R. L.

Lilova, W. Gao, E. Santiso, M. Daniele and S. Menegatti, *J. Mater. Chem. B*, 2020, **8**, 3852–3868.
222 M.-H. Shin, E.-Y. Park, S. Han, H. S. Jung, D. H. Keum, G.-H. Lee, T. Kim, C. Kim, K. S. Kim, S. H. Yun and S. K. Hahn, *Adv. Healthc. Mater.*, 2019, **8**, 1801036.
223 S. Wang, K. Li, Y. Chen, H. Chen, M. Ma, J. Feng, Q. Zhao and J. Shi, *Biomaterials*, 2015, **39**, 206–217.
224 W. Yin, L. Yan, J. Yu, G. Tian, L. Zhou, X. Zheng, X. Zhang, Y. Yong, J. Li, Z. Gu and Y. Zhao, *ACS Nano*, 2014, **8**, 6922–6933.
225 M. Xie, N. Yang, J. Cheng, M. Yang, T. Deng, Y. Li and C. Feng, *Colloids Surfaces B Biointerfaces*, 2020, **187**, 110631.
226 Z. Fu, G. R. Williams, S. Niu, J. Wu, F. Gao, X. Zhang, Y. Yang, Y. Li and L.-M. Zhu, *Nanoscale*, 2020, **12**, 14739–14750.
227 A. Sundaram, J. S. Ponraj, J. S. Ponraj, C. Wang, W. K. Peng, R. K. Manavalan, S. C. Dhanabalan, H. Zhang and J. Gaspar, *J. Mater. Chem. B*, , DOI:10.1039/d0tb00251h.
228 M. Qiu, D. Wang, W. Liang, L. Liu, Y. Zhang, X. Chen, D. K. Sang, C. Xing, Z. Li, B. Dong, F. Xing, D. Fan, S. Bao, H. Zhang and Y. Cao, *Proc. Natl. Acad. Sci.*, 2018, **115**, 501–506.
229 S. M. Sharker, *Int. J. Nanomedicine*, 2019, **Volume 14**, 9983–9993.
230 C. Martín, K. Kostarelos, M. Prato and A. Bianco, *Chem. Commun.*, 2019, **55**, 5540–5546.
231 P. Wick, A. E. Louw-Gaume, M. Kucki, H. F. Krug, K. Kostarelos, B. Fadeel, K. A. Dawson, A. Salvati, E. Vázquez, L. Ballerini, M. Tretiach, F. Benfenati, E. Flahaut, L. Gauthier, M. Prato and A. Bianco, *Angew. Chemie Int. Ed.*, 2014, **53**, 7714–7718.
232 S. Mateti, C. S. Wong, Z. Liu, W. Yang, Y. Li, L. H. Li and Y. Chen, *Nano Res.*, 2018, **11**, 334–342.
233 K. Kostarelos and K. S. Novoselov, *Science (80-.).*, 2014, **344**, 261–263.
234 J. Park, S. Park, S. Ryu, S. H. Bhang, J. Kim, J.-K. Yoon, Y. H. Park, S.-P. Cho, S. Lee, B. H. Hong and B.-S. Kim, *Adv. Healthc. Mater.*, 2014, **3**, 176–181.
235 B. Ma, C. Martín, R. Kurapati and A. Bianco, *Chem. Soc. Rev.*, 2020, 16–18.
236 D. A. Jasim, S. Murphy, L. Newman, A. Mironov, E. Prestat, J. McCaffrey, C. Ménard-Moyon, A. F. Rodrigues, A. Bianco, S. Haigh, R. Lennon and K. Kostarelos, *ACS Nano*, 2016, **10**, 10753–10767.
237 T. Liu, C. Wang, X. Gu, H. Gong, L. Cheng, X. Shi, L. Feng, B. Sun and Z. Liu, *Adv. Mater.*, 2014, **26**, 3433–3440.
238 IT Crew, Graphene Flagship - Health and Environment.